This paper reports results of experiments where pinonaldehyde, a product of atmospheric reactions of biogenic emissions, is photolyzed in a large outdoor environmental chamber in the presence and absence of an OH radical scavenger. The decay of pinonaldehyde, formation of formaldehyde, acetone, and ozone, and levels of OH and HO2 were monitored during the irradiations. However, there were no data on more complex organic products that may give more direct information on the mechanisms. Although results of only one experiment of each type were reported so reproducibility was not tested, this laboratory has a reputation for high quality data in well characterized experiments, and these appear to be no exception. It was found that pinonaldehyde photolyzed significantly more rapidly butyraldehyde, which is what is assumed in MCM and other mechanisms for higher aldehydes. The product and radical levels observed were not consistent with MCM predictions even after the pinonaldehyde photolysis rate was adjusted, and a more complex mechanism proposed by Fantechi et al (2002) (FAN) gave somewhat better predictions in some respects and somewhat worse in others. No mechanism was presented that was consistent with all the data.

This paper makes a contribution to our understanding of this important biogenic com-pound that should ultimately improve our ability to model its atmospheric impacts, and should be published. The measurement of the photolysis rate is an important contribution. On the other hand, this work certainly does not resolve uncertainties concerning details of the reaction pathways and the products formed – tests against formaldehyde data and acetone measurements (or lack thereof) are not very definitive because of the many way these small compounds could be formed. The problems fitting the radical data were examined in sensitivity calculations but not really resolved. Nevertheless, these results provide additional data that will be useful for understanding these mechanisms.

Although I recommend that this paper be accepted for publication, I have several comments and suggestions that the authors should consider before finalizing this paper.

We would like to thank the reviewer for reviewing our manuscript and providing helpful comments.

Comment 1: *Figure 1 shows how the major first-generation photolysis and OH reactions of pinonaldehyde are represented in the MCM and FAN models, and is the only place where the reader is informed of the structure of pinonaldehyde, which many readers won't know without looking it up, and of the various intermediates that are otherwise referenced in the text only with obscure MCM or FAN names. This figure is near the end of the manuscript in the review copy, but it needs to be at the very start of the published version so readers can more easily see the chemistry that is actually being discussed. Either that or have a very small figure near the beginning giving the structures being discussed.*

Response: We agree with the referee that Figure 1 should be placed early in the manuscript as part of the introduction. This will be done during the typesetting process for the final version for ACP.

Comment 2: *Although the FAN mechanism shown on Figure 1 is an improvement over MCM in that it considers more of the possible processes, it has some omissions that were not adequately considered in the sensitivity calculations. The paper mentioned that new data indicate that some peroxy radicals undergo unimolecular H-shift reactions, which is overlooked in both MCM and FAN, and the did sensitivity calculations (S1) showing the effect of assuming all those formed in the OH reaction rapidly react forming HO2. However, while the available data and estimates suggest that these H-shifts are fast for peroxy radicals with HCO- groups such as PINALO2, FAN_D1, and Fan_G1, there are no sufficiently labile abstractable H atoms for such reactions of C96CO3, which is formed about 60% of the time in the FAN model, or for the C96O2 radical that it forms. In addition, the reactions subsequent to the initial H-shifts are estimated to form another peroxy radical that converts NO to NO2, and it is not clear that this is included in the sensitivity calculation. If they did it was not stated, and they need to include a supplementary table giving the S1 mechanism, as they do with the FAN mechanism.*

Response: In the S1 mechanism only hypothetical isomerization reactions of the initial RO_2 radicals (C96CO3, FAN_D1, PINALO2, and FAN_G1) were tested. No subsequent chemistry of the isomerization products was considered. We added an additional table (see Table S1) in the Supplement with reactions considered in the S1 mechanism to clarify this.

In a new sensitivity run (S1_mod) only isomerization of RO_2 radicals with a –HCO group (FAN_D1, PINALO2, and FAN_G1) was tested. These RO_2 radicals are formed with a yield of 39 %. Therefore, HO_2 concentrations in the beginning of the experi-

ment are reduced by a factor of 2 compared to S1 where the isomerization of all initial RO_2 leads to the formation of HO_2. The reduced HO_2 concentrations agree with observations at the start of the photooxidation, but show the same temporal trend as S1.

We add on p14 l19:"However, only FAN_D1, PINALO2, and FAN_G1 have an aldehyde group with a hydrogen that can be easily abstracted (see Supplementary material)." We add the following part as a new section ("Sensitivity study S1 and additional sensitivity tests") to the Supplement:
"In S1 the impact of hypothetical isomerization reactions of all 4 initially formed RO_2 radicals on model results was tested. Reactions shown in Tab. S1 were added to the model based on Fantechi et al. (2002). Possible isomerziation reactions in later stages of the mechanism were not tested.

Table S1. Overview of added reactions for sensitivity run S1.

reaction	reaction rate constant
C96CO3 $\rightarrow$ HO_2	$0.1\,\mathrm{s}^{-1}$
PINALO2 $\rightarrow$ HO_2	$0.1\,\mathrm{s}^{-1}$
FAN_D1 $\rightarrow$ HO_2	$0.1\,\mathrm{s}^{-1}$
FAN_G1 $\rightarrow$ HO_2	$0.1\,\mathrm{s}^{-1}$

However, only PINALO2, FAN_D1, and FAN_G1 have an aldehyde group with a hydrogen that can be easily abstracted. An additional sensitivity study (S1_mod) was performed that includes only isomerization reactions of these 3 RO_2 applying the same reaction rates used for S1. Figure S1 shows the calculated HO_2 and OH time series together with results from S1, model base case (MCM_a), and modified mechanism by Fantechi et al. (2002) (FAN_a).

Figure S1. Model sensitivity studies of the impact of potential additional HO_2 formation by unimolecular RO_2 reactions of all 4 initial RO_2 (S1) and for RO_2 radicals with a –HCO group (S1_mod). The sensitivity test S1_mod_hv extends S1_mod by an additional photolysis of isomerization products. In addition, the model base case (MCM_a) and the case using the mechanism by Fantechi et al. (2002) (FAN_a) are shown. Grey shaded areas indicate times when the chamber roof was closed.

PINALO2, FAN_D1, and FAN_G1 are formed with a total yield of 39 %. Therefore, HO_2 concentrations in the beginning of the experiment are reduced by a factor of 2 compared to S1 where the isomerization of all initial RO_2 leads to the formation of HO_2. The reduced HO_2 concentrations agree with observations at the start of the photooxidation, but show the same temporal trend as in model run S1 over the course of the experiment. This leads to an increasing model-measurement discrepancy of HO_2 concentrations of a factor of up to 3. Consistently, OH concentrations are reduced by a factor of 2 compared to S1."

Comment 3: It is quite likely that the MCM and FAN mechanisms are underestimating radical input from photolyses of secondary products. If the dicarbonyl parent compound photolyzes faster than expected based on simpler monocarbonyls, that's

likely to be true for the many dicarbonyl products as well. They found that increasing photolysis rates to those for glyoxal did not increase radical levels sufficiently, and they had to increase them to that of NO2 (a rather extreme level that is not really reasonable) to get the radicals to the observed levels, and then it greatly overestimates initial HO2 radicals (Model S2). However, if the H-shift isomerizations of peroxy radicals with -HCO groups are indeed as fast as expected, then it is possible that peroxy acids with additional carbonyl groups may well be formed in up to 50% yields. These bifunctional compounds probably photolyze more rapidly than simple peroxy acids, and maybe more rapidly than glyoxal. This possibility would be worth examining.

Response: Following the suggestion of the referee, we did additional sensitivity runs with isomerization of RO_2 with a –HCO group followed by photolysis of the isomerization products with a photolysis frequency that is 2 times faster than the photolysis frequency of glyoxal. The photolysis of isomerization products leads to additional HO_2 production compared to the sensitivity run with only isomerization (Fig. S1, S1_mod) and reduces the HO_2 model-measurement discrepancy especially at later times in the experiment. The sensitivity test is able to reproduce measured OH concentrations within the measurement uncertainty. The result of this sensitivity run (S1_mod_hv) is now included in the Supplement. We add to the manuscript on p15 l3: "Another possibility is that the fast H-shift isomerization of RO_2 radicals (see Supplement) leads to the formation of peroxy acids with additional carbonyl functions in high yields. As discussed above, these bi-functional compounds could photolyse faster than currently implemented in the mechanism. A sensitivity test (S1_mod_hv, see Supplement) was performed that includes isomerization of RO_2 with a –HCO group. Products are assumed to photolyse with a photolysis rate that is 2 times higher than that of glyoxal. Implementation of these reactions leads to HO_2 concentrations that are increased by up to 60 % compared to the sensitivity run that includes only isomerization reactions. Calculated HO_2 concentrations underestimate measurements by factor of 2. The sensitivity test reproduces measured OH concentrations within the measurement uncertainty."

Comment 4: A major conclusion of this study is that "pinonaldehyde photolyzes faster than MCM predicts". That is true, but it is more to the point, and more meaningful to the photochemical community in general, to convey this as "pinonaldehyde photolyzes faster than simple aldehydes like butyraldehyde". This is because the MCM website indicates MCM assumes that all compounds like this photolyze as rapidly as buturaldehyde. The fact that this is not true has implications for all mechanisms and photochemistry in general.

Response: We add on p11 l23: "The pinonaldehyde photolysis is faster than n-butanal because of its two carbonyl functions. This might be valid for other bi-carbonyl compounds that have non-conjugated carbonyl functions, so that the use of the n-butanal photolysis frequency could systematically underestimate the photolysis frequencies of these compounds. However, the high quantum yield close to unity could also be a specific property of pinonaldehyde that might not apply for the photolysis of other bi-carbonyl species."

Comment 5: I am a bit uncomfortable with using models constrained to fit measured O3, NO, and NO2 when evaluating a mechanism's ability to predict HO2 radical levels. This is be-cause the rapid photostationary state reactions involving O3, NO, and NO2 require that the total rate of all peroxy + NO reactions be approximately equal the differences between the rates of the fast photolysis of NO2 and the fast reaction of O3 with NO, which are much larger in magnitude than the peroxy rates. It seems to me that this might cause small measurement uncertainties in NO, NO2 or O3 to have large effects on artificial radical sources and sinks required to for this constraint to hold. It may be valid the way they did this, but more discussion may be needed. It would be more straightforward and understandable if they could constrain to as few measurements as possible when evaluating mechanisms, and preferably only using reaction conditions such as jNO2. Why not just constrain just one of the reactant predictions, and let the others fall where the mechanism tells you?

Response: One aim of our study is the understanding of HO_x radical concentrations in the pinonaldehyde photooxidation. Because the loss of HO_2 in the reaction with NO is a major source of OH, model results could have led to wrong conclusions, if the NO concentration in the model did not match observations. The measurement uncertainties of O_3, NO, and NO_2 are very small (5 %). Therefore, most accurate results with respect to the turnover rates of radicals are obtained, if measured concentrations are used.

In contrast, not constraining the model to measurements would require an accurate description of all chamber NO sources. The major source of NO in the chamber is photolysis of HONO that is formed on the Teflon wall of the sunlit chamber.

Unfortunately, HONO was only measured in one of these experiments, so that the NO source cannot be accurately described in the model.

We add the reason for the constrains to the manuscript on p8 l12: "These constrains were used because chamber NO sources cannot be modeled accurately and therefore could lead to wrong conclusions in the analysis of turnover rates of radicals."

Comment 6: *The ratio of rate constants used in the model for the reactions of peroxy radicals with HO2 vs. NO may also affect model predictions of HO2. Has this been looked into? These rate constants have not been measured, and estimates based on rate constants for simpler radicals may be an oversimplification.*

Response: We performed an additional sensitivity run based on the Fantechi et al. (2002) mechanism with a reaction rate constant for $RO_2 + NO$ (KRO2NO) that is faster by a factor 2 compared to the MCM. Results of this sensitivity runs are shown in Fig. S2. The enhanced reaction rate leads to an increased fraction of RO_2 reacting with NO instead of HO_2. As a result, HO_2 concentrations are enhanced by approximately 50 % compared to the model run FAN_a. However, HO_x concentrations are again underestimated compared to measurements and the sensitivity run cannot reproduce the HO_2 concentration time behaviour from observations.
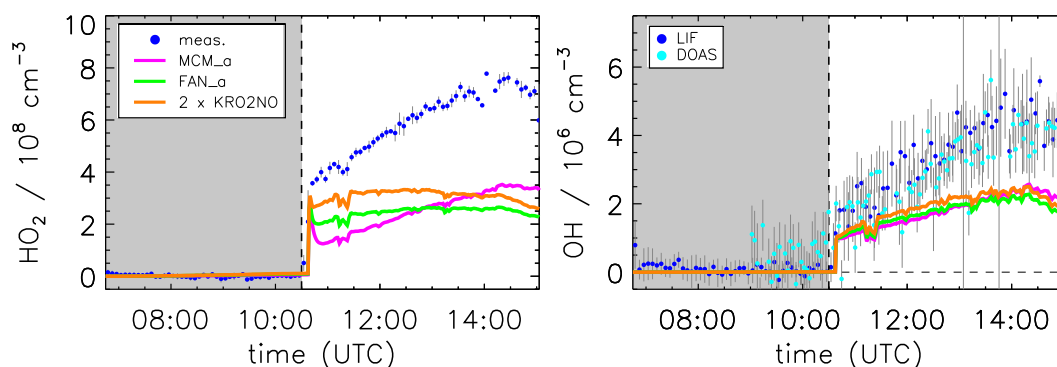
Figure S2. Model sensitivity run with modified reaction rate of 2xKRO2NO. The modified reaction rate constant was applied to all RO_2 that were introduced by the model modifications based on Fantechi et al. (2002). Grey shaded areas indicate times when the chamber roof was closed.

Figure S2 is added to the Supplement. We add to the manuscript on p13 l21: "Modeled HO_2 concentrations could be affected by the use of general reaction rate constants for reactions of RO_2 with HO_2 and NO (KRO2HO2 and KRO2NO), respectively. This might be an oversimplification for highly functionalized compounds. A sensitivity test (see Supplement) with an enhanced reaction rate for $RO_2 + NO$ reactions of $2\times$ KRO2NO in the modified mechanism by Fantechi et al. (2002) was performed. As a result, the fraction of RO_2 reacting with NO instead of HO_2 is increased. This leads to an enhanced HO_2 concentration of approximately 50 % compared to the model run FAN_a. However, HO_x concentrations are again underestimated compared to measurements and the sensitivity run cannot reproduce the HO_2 concentration time behaviour from observations."

Minor comments: *I have the following minor formatting comments on the figures:*
(1) Most of the figures are not suitable for presentation in black and white.
Atmospheric Chemistry and Physics is an online journal providing coloured PDF documents. Therefore, coloured figures are very common. We do not have the feeling that there is need to optimize the figures for black and white printing.

(2) The species whose concentrations are being plotted should be shown more conspicuously. Right now, this information is only given in very tiny font on the reaction labels.
The names of species shown in Figure 2 and 3 were added in larger font on each sub-plot. The size of the axis labelling was

increased in Figures 4-7.

(3) The FAN_a result is not shown in the top plot of Figure 6, probably because it is exactly the same as MCM_a. Perhaps it should be stated in the caption that they are the same.
We changed the figure as suggested.

(4) On figure 8, the color shown for MCM on the legend (red) does not match the color on the plots (pink).
We changed the figure to better match colors.

Anonymous Referee #2

The paper reports experiments on pinonaldehyde oxidation, conducted in the SAPHIR chamber in Juelich. In one experiment, the oxidation was initiated exclusively by photolysis, in the other, pinonaldehyde reacted primarily with OH. The chamber is highly instrumented and has been very well characterized. The experiments were conducted at low NO and concentrations of pinonaldehyde, HCHO, acetone, NO, NO2, O3, HONO,OH and HO2 were measured, together with the actinic flux outside the chamber, over a period of ~4 h. The results were compared with simulations based on the master chemical mechanism (MCM) and on a theoretically based alternative. The results show that there are significant deficiencies in both these mechanisms and suggestions for revisions are made.
The results and the analysis make a significant contribution to improving our under-standing of an aspect of the atmospheric oxidation of α-pinene – the key pinonaldehyde precursor – and should be published. The authors should consider the following points in a revision of the manuscript.

We would like to thank the reviewer for reviewing our manuscript and providing helpful comments.

Comment 1: *It is disappointing that only two experiments were conducted, one on photolysis and the other on OH oxidation, so there is no testing of the observations and interpretation via variation, for example, of the initial [NO]. I appreciate that the experiments are complex and resource-intensive, but some comment might be made on the implications of this limitation. In addition, the authors should comment on the strong variations in [HO2] in the photolysis experiment(Figs 2 and 6) which is greater than the experimental uncertainty and is not reproduced in the models. The afternoon decrease is at least partly explained by a decrease in j(pinonaldehyde), but there are other variations also. The variability is much less pronounced in the OH initiation experiments.*
Response: Pinonaldehyde has a low vapour pressure and is a very sticky compound. Therefore, it was complicated to transfer pinonaldehyde into the chamber. In total 4 experiments were performed. Unfortunately, only in 2 experiments shown in this manuscript the transfer of pinonaldehyde into the chamber was successful. In general, experiments in the SAPHIR chamber are very time-consuming and require a large team to measure trace gas concentrations and analyse data. As much as we agree that a larger set of experiments were beneficiary, we could not perform more experiments at different conditions for this work. We nevertheless think that results are important to report.
We add in the manuscript, p12 l18 to discuss the variations of HO_2 in the photolysis experiment: "Unfortunately, between 11:30 and 14:00 experimental problems occurred in the HO_2 measurements. Neither NO measurements nor photolysis frequencies showed any features that could explain the decrease in the HO_2 concentration. The exact reason of the HO_2 variations remains unclear and the uncertainty of HO_2 measurements is likely higher (50 %) for this period."

Comment 2: *It would be helpful if there were an indication of just how important pinonaldehyde is in the oxidation of α-pinene. There are a number of routes to pinonaldehyde and their importance depends on conditions, so this is not an easy request to satisfy, but some indication under relevant conditions would be useful, together with an indication of the dominant routes. It is suggested that the yield is small in the field campaigns discussed on p16. Under what conditions is pinonaldehyde production important? Some information on the transmission of the chamber walls and its impact on the spectral distribution should be made. The maximum in the pinonaldehyde spectrum lies below 300 nm, while the absorption has fallen to half its maximum*

value at ∼310 nm, so the photolysis wavelengths and rate could be impacted significantly by the wall transmission and its wavelength dependence.

Response: Previous laboratory studies reported a broad range of pinonaldehyde yields (5-87 %, see Rolletter et al., 2019, and references therein) in the photooxidation of α-pinene. In the α-pinene photooxidation by OH, initially 3 different RO_2 are formed and 2 of them eventually form pinonaldehyde. As currently implemented in the MCM pinonaldehyde is formed with a total yield of 84 %. In contrast, a theory based study by Vereecken et al. (2007) suggests a different branching ratio of initial RO_2 and additional reaction channels which lead in total to pinonaldehyde yields of 60 % for low atmospheric NO conditions (≤ 1 ppbv NO). For laboratory conditions with high NO mixing ratios (≥ 50 ppbv NO), the pinonaldehyde yield of their mechanism is reduced to 36 %. Our previous study (Rolletter et al., 2019) showed that further adjustment of the initial RO_2 branching ratio in a mechanism based on Vereecken et al. (2007) was necessary to explain the low pinonaldehyde yield of 5 % for conditions similar to the experiments discussed here (≤ 0.3 ppbv NO). A similar change in RO_2 branching ratios was found in an experimental study by Xu et al. (2019). The current lack of ambient measurement data makes it difficult to explain when the pinonaldehyde formation becomes important.

We add on p3 l19: "In the α-pinene photooxidation, initially 3 different peroxy radicals (RO_2) are formed and 2 of them eventually form pinonaldehyde."

In addition, we add on p3 l30: "As currently implemented in the Master Chemical Mechanism (MCM, 2017; Jenkin et al., 1997; Saunders et al., 2003) pinonaldehyde is formed with a total yield of 84 %. In contrast, a theory based study by Vereecken et al. (2007) suggested a different branching ratio of initial RO_2 and additional reaction channels which lead in total to pinonaldehyde yields of 60 % for low atmospheric NO conditions (≤ 1 ppbv NO). Our previous study (Rolletter et al., 2019) showed that further adjustment of the initial RO_2 branching ratio in a mechanism based on Vereecken et al. (2007) was necessary to explain the low measured pinonaldehyde yield of 5 % for conditions similar to the experiments discussed here. A similar change in RO_2 branching ratios was found in an experimental study by Xu et al. (2019)."

Compared to outdoor conditions actinic flux densities and photolysis frequencies inside the chamber are lower by about 40 % mostly because of shading effects and the transmission of the chamber film. The wavelength dependence of the transmittance of the Teflon was investigated in the laboratory and is part of the model used to calculate photolysis frequencies inside the chamber (Bohn and Zilken, 2005). However, the change of the spectrum is minor, i.e. the spectral distribution inside the chamber is very similar to outside.

We rephrase on p7, l6: "The direct and diffuse actinic flux densities are used as input for a model which calculates mean chamber spectra by taking into account the time-dependent effects of shadings of the chamber steel frame and the transmittance of the Teflon film which is > 0.8 in the complete solar spectral range (Bohn and Zilken, 2005)."

Comment 3: *The photolysis experiment demonstrates that the MCM significantly underestimates the photolysis rate and this is corrected in the paper, which also demonstrates that the yields of acetone and HCHO are substantially overestimated in the MCM. This is addressed by using the mechanism developed by Fantechi et al to describe the reactions of the oxy radical formed from pinonaldehyde photolysis. As pointed out in the paper, their simulations did not include the subsequent reactions of the main products of this reaction, 4-Hydroxynorpinonaldehyde, which will react further and will also be photolyzed, almost certainly on the timescales of the experiment. It is suggested that it might be a further source of HO2, but it could also be a source of HCHO and acetone. Further discussion, possibly ruling out this possibility, and some suggestion of the likely products is essential. The estimated experimental yield of acetone shown in Fig 4 is initially negative, which is difficult to understand. Some explanation is needed.*

Response: Corrections of acetone concentrations were applied to experimentally derive the product yield. This includes losses by the reaction with OH and by dilution. Negative yields can arise when the chamber source parameterisation overestimates the acetone formation. This adds to the uncertainty of the yield calculation. The main uncertainty of the yield (20 %) is indeed caused by the uncertainty of the chamber source in addition to the uncertainty that is calculated from the precision of data shown in Fig. 4.

We changed the caption of Figures 4 & 5 to mention that the additional uncertainty from the chamber source is not shown. We add on p11 l34: "Initial acetone yield values are negative because of the high uncertainty in the corrections that are applied in the yield calculation. In the beginning of an experiment, only small amounts of products are formed which leads to a large uncertainty, so that negative values are not significant."

In our response to comment 4 more information is given about potential products in the degradation of 4-hydroxinorpinon-aldehyde. A sensitivity study was performed to test if the channels II, III, and IV of the reaction of pinonaldehyde + OH have the potential to close the gap between modeled and measured acetone and formaldehyde concentrations in the OH photooxidation experiment. Results can be seen in Fig. S3. The additional acetone and HCHO sources can reproduce observations in the first half of the experiment within the measurement uncertainty when contributions from OH reactions of product species are small. In later stages of the experiment, acetone and formaldehyde concentrations are underestimated by the sensitivity model run. Additional acetone and HCHO formation from further degradation of oxidation products not included in the MCM could explain the model-measurement discrepancy. In the photolysis experiment with OH scavenger present, measured acetone and formaldehyde concentrations could be reproduced by the model based on Fantechi et al. (2002). In this case, additional 4-hydroxynorpinonaldehyde photolysis forming acetone and HCHO would lead to an overestimation of modeled acetone and HCHO concentrations.
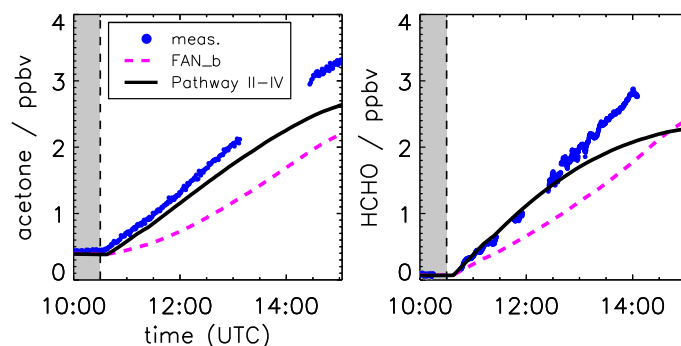
Figure S3. Measured and modeled formaldehyde and acetone mixing ratios for the experiment without OH scavenger. All model runs were done with measured photolysis frequencies for pinonaldehyde and with HO_2 constrained to measurements. Model runs were done using modifications described in Fantechi et al. (2002). For the model run shown in black an additional HCHO and acetone formation in pathways II, III, and IV is assumed.

Figure S3 and a description of the sensitivity test are added to the Supplement.

Comment 4: The MCM and the Fantechi mechanism cannot explain the yields of HCHO or acetone in the OH initiated oxidation and the paper shows that they seriously underestimate HO2. Two attempts are made to understand the deficiencies, based on isomerization of RO2 species via an autoxidation mechanism and photolysis of intermediates. The latter appears to provide a better explanation. It is disappointing that a more considered analysis isn't given, especially since the senior author of the Fantechi paper leads the theoretical kinetics group at Juelich. I am not suggesting that major calculations are appropriate at this stage, but more informed comments and suggestions of the way forward might be made (e.g. amplifying the comment at lines 8,9 on p 14).

Response:

We did further test to explain the unknown HO_2 source but could not find any better explanations than discussed in the manuscript. The theory derived pinonaldehyde degradation scheme by Fantechi et al. (2002) has 4 competitive channels with a large uncertainty for the site specificity of the initial OH attack. This could affect the products distrubution. Our analysis relies completely on the product distribution that is prescribed by the model. Quantification of specific products would have helped to better constrain the used mechanism. In the photooxidation experiment a huge variety of different products is formed so that the missing HO_2 source cannot be easily explained by the subsequent chemistry of one species. For example, a new degradation mechanism for 4-hydroxynorpinonaldehyde deduced from structure–activity relationship (SAR; Kwok and Atkinson, 1995; Vereecken and Peeters, 2009; Vereecken and Nozière, 2020) was tested. 4-hydroxynorpinonaldehyde is formed as major product in the photooxidation experiment with an overall yield of approximately 25 % and no subsequent chemistry was considered in the MCM model and the modified Fantechi mechanism. However, the impact of the tested subsequent chemistry

of 4-hydroxynorpinonaldehyde on the HO_2 formation was small ($\leq 10\%$) compared to the modified mechanism by Fantechi et al. (2002).

The effort for theoretical calculations of the chemistry is very high and cannot be done for all experiments that we perform in the chamber. In addition, no products measurements are available that would help to verify results from theoretical calculations. Therefore, the discussion is limited to provide hints, what will need to be looked into in the future.

We add on p15 l10: "No subsequent chemistry of 4-hydroxynorpinonaldehyde is included in the mechanism so far. In the experiment here 4-hydroxynorpinonaldehyde is formed with an overall yield of approximately 25%. 4-hydroxynorpinon-aldehyde is highly functionalized and RO_2 radicals formed in its degradation could undergo fast isomerization reactions. For a sensitivity run (S3, see Supplement) a mechanism was deduced with the structure–activity relationship (SAR; Kwok and Atkinson, 1995; Vereecken and Peeters, 2009; Vereecken and Nozière, 2020) method. However, the impact of the tested 4-hydroxynorpinonaldehyde degradation scheme on the HO_2 formation was small ($\leq 10\%$) compared to the modified mechanism by Fantechi et al. (2002). Unfortunately, no measurements of stable oxidation products other than acetone and HCHO were available. Without further product measurements the whole analysis discussed here relies on product distribution prescribed by the models. Further experiments that measure oxidation products and yields could help to better constrain branching ratios in degradation mechanisms. In addition, theoretical studies could investigate subsequent degradation schemes of major products in more detail."

We add a section to the Supplement describing the tested degradation mechanism of 4-hydroxynorpinonaldehyde: "In the used mechanism based on Fantechi et al. (2002) 4-hydroxynorpinonaldehyde was formed as main product with an overall yield of approximately 25% but no subsequent chemistry was considered in the MCM model and the modified Fantechi mechanism. To investigate if the subsequent chemistry of this product has the potential to partly explain the missing HO_2 source a mechanism was deduced from structure–activity relationship (SAR; Kwok and Atkinson, 1995; Vereecken and Peeters, 2009; Vereecken and Nozière, 2020).
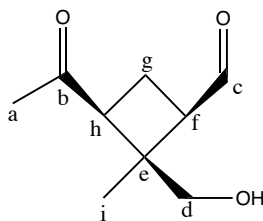
Figure S4. Structure of 4-hydroxynorpinonaldehyde and C-atom labeling.

The 4-hydroxynorpinonaldehyde structure is shown in Fig. S4. Reaction rate constants for the H-abstraction by OH were estimated based on Kwok and Atkinson (1995) and are shown in Table S2.

Table S2. Reaction rate constants for H-abstraction by OH for different carbon atoms based on Kwok and Atkinson (1995).

C-atom	reaction rate constant	fraction
c	1.69×10^{-11} cm^3 s^{-1}	79%
d	3.27×10^{-12} cm^3 s^{-1}	15%
f	5.43×10^{-13} cm^3 s^{-1}	3%
g	2.62×10^{-13} cm^3 s^{-1}	1%
h	5.43×10^{-13} cm^3 s^{-1}	3%

A simplified mechanism of the subsequent degradation of 4-hydroxynorpinonaldehyde is shown in Fig. S5. An overview of added reactions is shown in Table S3. Reaction rates were based on Vereecken and Peeters (2009); Vereecken and Nozière
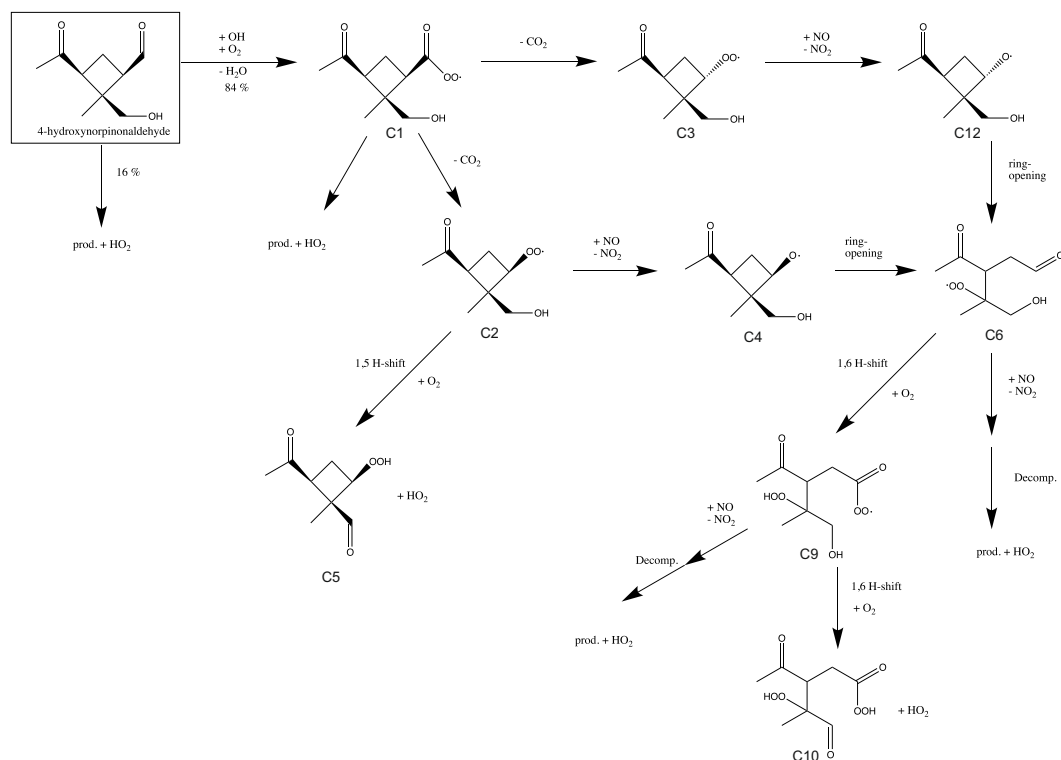
Figure S5. Simplified mechanism of the subsequent degradation of 4-hydroxynorpinonaldehyde. The mechanism is deduced from SAR. For details see text. $RO_2 + HO_2$ reactions and $RO_2 + NO$ reactions that form nitrates are not shown.

(2020). Only the main reaction branches ($\geq 5\%$) were investigated. The mechanism was constructed using SAR described in Jenkin et al. (1997). For all $RO_2 + NO$ reactions the standard reaction rate from MCM (KRO2NO) and an organic nitrate yield of 23 % was used. $RO_2 + HO_2$ reactions were included as described for the modified mechanism based on Fantechi et al. (2002). The photolysis frequency of pinononaldehyde was used for the photolysis of formed hydroperoxides (ROOH).

H-abstraction by OH mainly occurs at the aldehyde group forming the peroxy radical C1. After a rapid CO_2 elimination, C1 forms C2 and C3 in equal amounts. C2 can undergo an 1,5 H-shift to form a stable hydroperoxy compound (C5) and HO_2. Alternatively, C2 can form the alkoxy radical C4 after reaction with NO. Similarly, C3 forms the alkoxy radical C12. Ring-opening of the 4-membered ring in both C4 and C12 leads to the formation of a peroxy radical C6. Subsequently, the main fraction (approximately 90 %) rearranges after an 1,6 H-shift to C9. C9 either undergoes an 1,6 H-shift forming C10 or forms an alkoxy radical that further decomposes to a stable product and HO_2.

A sensitivity run (S3) using the degradation scheme of 4-hydroxynorpinonaldehyde was performed and results can be seen in Fig. S6. The modifications have only a small effect on HO_2 and OH concentrations. In the second half of the experiment the degradation of pinonaldehyde oxidation products becomes more relevant and additional HO_2 is formed by the 4-hydroxynorpinonaldehyde degradation scheme. However, the effect on the HO_2 concentration is small and HO_2 concentrations are increased by up to 10 % compared to FAN_a."
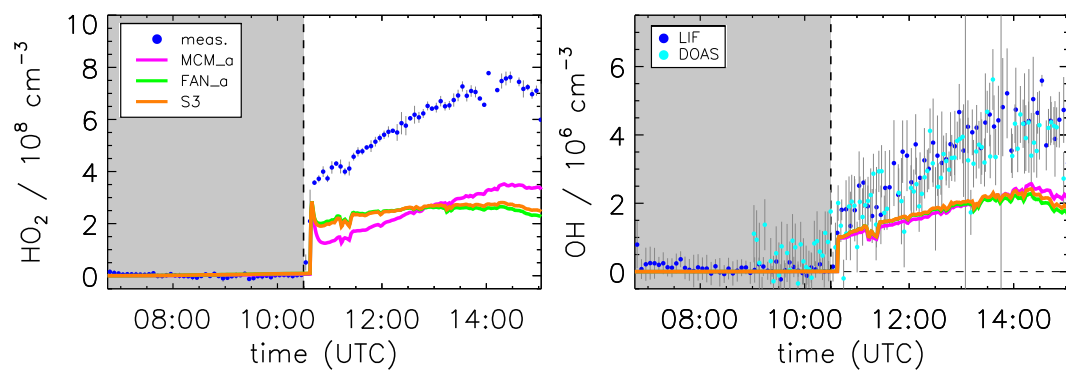
Figure S6. Model sensitivity study of the impact of a 4-hydroxynorpinonaldehyde degradation mechanism (S3) compared to the model base case (MCM_a) and the case using the mechanism by Fantechi et al. (2002) (FAN_a). Grey shaded areas indicate times when the chamber roof was closed.

Table S3. Extended mechanism for the further degradation of 4-hydroxynorpinonaldehyde used for sensitivity test S3. For details see text. All nitrate species are lumped as one species RNO3.

reaction	reaction rate constant
NORPINALOH + OH → C1	$1.69 \times 10^{-11}\,\mathrm{cm^3\,s^{-1}}$ [a]
NORPINALOH + OH → D1 + HO$_2$	$3.27 \times 10^{-12}\,\mathrm{cm^3\,s^{-1}}$ [a]
NORPINALOH + OH → F1 + HO$_2$	$5.43 \times 10^{-13}\,\mathrm{cm^3\,s^{-1}}$ [a]
NORPINALOH + OH → G1 + HO$_2$	$2.62 \times 10^{-13}\,\mathrm{cm^3\,s^{-1}}$ [a]
NORPINALOH + OH → H1 + HO$_2$	$5.43 \times 10^{-13}\,\mathrm{cm^3\,s^{-1}}$ [a]
NORPINALOH + hν → C2 + HO$_2$	j_{PINAL}
C1 → C2 + CO$_2$	KDEC[b]
C1 → C3 + CO$_2$	KDEC[b]
C1 → prod. + HO$_2$	$9.16 \times 10^{-2}\,\mathrm{s^{-1}}$
C1 + NO → C1O + NO$_2$	0.77*KRO2NO[c]
C1 + NO → RNO3	0.23*KRO2NO[c]
C1 + HO$_2$ → C1OOH	KRO2HO2[d]
C1OOH + OH → C1	$1.3 \times 10^{-11}\,\mathrm{cm^3\,s^{-1}}$
C1OOH + hν → C1O + OH	j_{PINAL}
C1O → prod. + HO$_2$	KDEC[b]
C2 + NO → C4 + NO$_2$	0.77*KRO2NO[c]
C2 + NO → RNO3	0.23*KRO2NO[c]
C2 → C5 + HO$_2$	$1.3 \times 10^{-2}\,\mathrm{s^{-1}}$
C2 + HO$_2$ → C2OOH	KRO2HO2[d]
C2OOH + OH → C2	$1.3 \times 10^{-11}\,\mathrm{cm^3\,s^{-1}}$
C2OOH + hν → C4 + OH	j_{PINAL}
C4 → C6	KDEC[b]
C6 → C9	$2.8 \times 10^{-1}\,\mathrm{s^{-1}}$
C6 + NO → C7 + NO$_2$	0.77*KRO2NO[c]
C6 + NO → RNO3	0.23*KRO2NO[c]
C6 + HO$_2$ → C6OOH	KRO2HO2[d]
C6OOH + OH → C6	$1.3 \times 10^{-11}\,\mathrm{cm^3\,s^{-1}}$
C6OOH + hν → C7 + OH	j_{PINAL}
C7 → C8 + ACETOL	KDEC[b]
C8 → prod. + HO$_2$	KDEC[b]
C9 → C10 + HO$_2$	$6.6 \times 10^{-4}\,\mathrm{s^{-1}}$
C9 + NO → C11 + NO$_2$	0.77*KRO2NO[c]
C9 + NO → RNO3	0.23*KRO2NO[c]
C9 + HO$_2$ → C9OOH	KRO2HO2[d]
C9OOH + OH → C9	$1.3 \times 10^{-11}\,\mathrm{cm^3\,s^{-1}}$
C9OOH + hν → C11 + OH	j_{PINAL}
C11 → C13 + HO$_2$	KDEC[b]
C3 + NO → C12 + NO$_2$	0.77*KRO2NO[c]
C3 + NO → RNO3	0.23*KRO2NO[c]
C3 + HO$_2$ → C3OOH	KRO2HO2[d]
C3OOH + OH → C3	$1.3 \times 10^{-11}\,\mathrm{cm^3\,s^{-1}}$
C3OOH + hν → C12 + OH	j_{PINAL}
C12 → C6 + HO$_2$	KDEC[b]

[a] value from Kwok and Atkinson (1995)
[b] value from MCM: KDEC= $1.0 \times 10^{6}\,\mathrm{s^{-1}}$ (MCM, 2017)
[c] value from MCM: KRO2NO= $2.7 \times 10^{-12}\exp(360\mathrm{K}/\mathrm{T})\,\mathrm{cm^3\,s^{-1}}$ (MCM, 2017)
[d] value from MCM: KRO2HO2= $2.91 \times 10^{-13}\exp(1300\mathrm{K}/\mathrm{T})\,\mathrm{cm^3\,s^{-1}}$ (MCM, 2017)

Minor comments:

What integrator was used in the simulations?
All model calculations were performed with FACSIMILE as solver.
We add this information in the manuscript (p8, l6): "FACSIMILE was used as solver for differential equations in the model calculations."

The English needs some attention (e.g. line 12, p12 should be rise (or increase wouldbe better); line 5, p13 replace "MCM like found in" with "MCM, such as the")
Changed as suggested.

Line 15, p15. Should be version 3.3.1.
Changed as suggested.

References

Bohn, B. and Zilken, H.: Model-aided radiometric determination of photolysis frequencies in a sunlit atmosphere simulation chamber, Atmos. Chem. Phys., 5, 191–206, https://doi.org/10.5194/acp-5-191-2005, 2005.

Fantechi, G., Vereecken, L., and Peeters, J.: The OH-initiated atmospheric oxidation of pinonaldehyde: Detailed theoretical study and mechanism construction, Phys. Chem. Chem. Phys., 4, 5795–5805, https://doi.org/10.1039/B205901K, 2002.

Jenkin, M. E., Saunders, S. M., and Pilling, M. J.: The tropospheric degradation of volatile organic compounds: A protocol for mechanism development, Atmos. Environ., 31, 81–104, https://doi.org/10.1016/S1352-2310(96)00105-7, 1997.

Kwok, E. S. C. and Atkinson, R.: Estimation of hydroxyl radical reaction rate constants for gas-phase organic compounds using a structure-reactivity relationship: An update, Atmos. Environ., 29, 1685–1695, https://doi.org/10.1016/1352-2310(95)00069-B, 1995.

MCM: Master Chemical Mechanism, http://mcm.leeds.ac.uk/MCM/, last access: 04 March 2020, 2017.

Rolletter, M., Kaminski, M., Acir, I. H., Bohn, B., Dorn, H. P., Li, X., Lutz, A., Nehr, S., Rohrer, F., Tillmann, R., Wegener, R., Hofzumahaus, A., Kiendler-Scharr, A., Wahner, A., and Fuchs, H.: Investigation of the α-pinene photooxidation by OH in the atmospheric simulation chamber SAPHIR, Atmos. Chem. Phys., 19, 11 635–11 649, https://doi.org/10.5194/acp-19-11635-2019, 2019.

Saunders, S. M., Jenkin, M. E., Derwent, R. G., and Pilling, M. J.: Protocol for the development of the Master Chemical Mechanism, MCMv3 (Part A): Tropospheric degradation of non-aromatic volatile organic compounds, Atmos. Chem. Phys., 3, 161–180, https://doi.org/10.5194/acp-3-161-2003, 2003.

Vereecken, L. and Nozière, B.: H migration in peroxy radicals under atmospheric conditions, Atmos. Chem. Phys., 20, 7429–7458, https://doi.org/10.5194/acp-20-7429-2020, 2020.

Vereecken, L. and Peeters, J.: Decomposition of substituted alkoxy radicals-part I: a generalized structure-activity relationship for reaction barrier heights, Phys. Chem. Chem. Phys., 11, 9062–9074, https://doi.org/10.1039/B909712K, 2009.

Vereecken, L., Müller, J. F., and Peeters, J.: Low-volatility poly-oxygenates in the OH-initiated atmospheric oxidation of α-pinene: impact of non-traditional peroxyl radical chemistry, Phys. Chem. Chem. Phys., 9, 5241–5248, https://doi.org/10.1039/B708023A, 2007.

Xu, L., Møller, K. H., Crounse, J. D., Otkjær, R. V., Kjaergaard, H. G., and Wennberg, P. O.: Unimolecular Reactions of Peroxy Radicals Formed in the Oxidation of α-Pinene and β-Pinene by Hydroxyl Radicals, J. Phys. Chem. A,, 123, 1661–1674, https://doi.org/10.1021/acs.jpca.8b11726, 2019.

Photooxidation of pinonaldehyde at ambient conditions investigated in the atmospheric simulation chamber SAPHIR

Michael Rolletter[1], Marion Blocquet[1,a], Martin Kaminski[1,b], Birger Bohn[1], Hans-Peter Dorn[1], Andreas Hofzumahaus[1], Frank Holland[1], Xin Li[1,c], Franz Rohrer[1], Ralf Tillmann[1], Robert Wegener[1], Astrid Kiendler-Scharr[1], Andreas Wahner[1], and Hendrik Fuchs[1]

[1]Institute of Energy and Climate Research, IEK-8: Troposphere, Forschungszentrum Jülich GmbH, Jülich, Germany
[a]now at: Ministère de l'Education Nationale et de la Jeunesse, 110 rue de Grenelle, 75357 Paris SP 07
[b]now at: Federal Office of Consumer Protection and Food Safety, Department 5: Method Standardisation, Reference Laboratories, Resistance to Antibiotics, Berlin, Germany
[c]now at: College of Environmental Sciences and Engineering, Peking University, Beijing, China

Correspondence to: Hendrik Fuchs (h.fuchs@fz-juelich.de)

Abstract. The photooxidation of pinonaldehyde, one product of the α-pinene degradation, was investigated in the atmospheric simulation chamber SAPHIR under natural sunlight at low NO concentrations (< 0.2 ppbv) with and without an added hydroxyl radical (OH) scavenger. With scavenger, pinonaldehyde was exclusively removed by photolysis, whereas without scavenger, the degradation was dominated by reaction with OH. In both cases, the observed rate of pinonaldehyde consumption was faster than predicted by an explicit chemical model, the Master Chemical Mechanism (MCM, version 3.3.1). In the case with OH scavenger, the observed photolytic decay can be reproduced by the model, if an experimentally determined photolysis frequency is used instead of the parameterization in the MCM. A good fit is obtained, when the photolysis frequency is calculated from the measured solar actinic flux spectrum, absorption cross-sections published by Hallquist et al. (1997), and an effective quantum yield of 0.9. The resulting photolysis frequency is 3.5 times faster than the parameterization in the MCM. When pinonaldehyde is mainly removed by reaction with OH, the observed OH and hydroperoxy radical (HO_2) concentrations are underestimated in the model by a factor of 2. Using measured HO_2 as a model constraint brings modeled and measured OH concentrations into agreement. This suggests that the chemical mechanism includes all relevant OH producing reactions, but is missing a source for HO_2. The missing HO_2 source strength of $(0.8 \text{ to } 1.5)\,\mathrm{ppbv\,h^{-1}}$ is similar to the rate of the pinonaldehyde consumption of up to $2.5\,\mathrm{ppbv\,h^{-1}}$. When the model is constrained by HO_2 concentrations and the experimentally derived photolysis frequency, the pinonaldehyde decay is well represented. The photolysis of pinonaldehyde yields 0.18 ± 0.20 formaldehyde molecules at NO concentrations of less than $200\,\mathrm{pptv}$, but no significant acetone formation is observed. When pinonaldehyde is also oxidized by OH under low NO conditions (maximum $80\,\mathrm{pptv}$), yields of acetone and formaldehyde increase over the course of the experiment from 0.2 to 0.3 and from 0.15 to 0.45, respectively. Fantechi et al. (2002) proposed a degradation mechanism based on quantum-chemical calculations, which is considerably more complex than the MCM scheme and contains additional reaction pathways and products. Implementing these modifications results in a closure of the model-measurement discrepancy for the products acetone and formaldehyde, when pinonaldehyde is degraded only by photolysis. In contrast, the underprediction of formed acetone and formaldehyde is worsened compared to model results by the MCM,

when pinonaldehyde is mainly degraded in the reaction with OH. This shows that the current mechanisms lack acetone and formaldehyde sources for low NO conditions like in these experiments. Implementing the modifications suggested by Fantechi et al. (2002) does not improve the model-measurement agreement of OH and HO_2.

1 Introduction

Globally, emissions of biogenic non-methane volatile organic compounds (NMVOCs) in the atmosphere are ten times higher than emissions of anthropogenic NMVOCs (Guenther et al., 2012). Of these emissions, monoterpenes (C10-compounds) represent approximately 15 % (Guenther et al., 2012) of the total emissions. Monoterpenes are mainly oxidized in the atmosphere by ozonolysis or their reaction with the hydroxyl radical (OH) during daytime. However, also oxidation by the nitrate radical (NO_3) during nighttime can be of importance enhanced by nocturnal monoterpene emissions (Calogirou et al., 1999; Atkinson and Arey, 2003). Oxidation products significantly contribute to the global production of, for example, acetone (Jacob et al., 2002). In addition, low-volatile organic oxidation products play an important role for the formation of secondary organic aerosol (SOA) (Kanakidou et al., 2000). The oxidation of monoterpenes and their oxidation products is also of importance for the tropospheric ozone production (Schwantes et al., 2020).

Field measurements indicate that there is a lack of understanding of the radical chemistry connected to the photooxidation of monoterpenes (e.g. Peeters et al., 2001; Capouet et al., 2004, and references therein). Hydroperoxy radical (HO_2) concentrations measured in environments dominated by monoterpenes are not well-understood by model calculations, for example in a campaign performed in the foothills of the Rocky Mountains (Kim et al., 2013) and in a boreal forest in Finland (Hens et al., 2014). In these campaigns, modeled HO_2 concentrations were lower by a factor of 2 and 2.5, respectively, compared to measurements. Also chamber studies, investigating the oxidation of α- and β-pinene gave higher HO_2 concentrations than model calculations suggest (Kaminski et al., 2017; Rolletter et al., 2019).

Among the monoterpenes, α-pinene is the most abundant one (Guenther et al., 2012). Pinonaldehyde is one of the first-generation oxidation products. In the α-pinene photooxidation, initially 3 different peroxy radicals (RO_2) are formed and 2 of them eventually form pinonaldehyde. Several field campaigns reported pinonaldehyde concentrations measured on filter samples (Kavouras et al., 1999; Alves et al., 2002; Boy et al., 2004; Cahill et al., 2006; Rissanen et al., 2006; Herckes et al., 2006; Plewka et al., 2006) or in the analysis of rain and snow samples (Satsumabayashi et al., 2001). Only few studies reported ambient gas phase concentrations of pinonaldehyde. Field studies in the San Bernardino National Forest, California (Yu et al., 1999) and the German Fichtelgebirge (Müller et al., 2006) reported pinonaldehyde concentrations in the gas phase of approximately 0.15 ppbv. Another study by Cahill et al. (2006) conducted in the Sierra Nevada Mountains of California measured 0.05 to 0.30 ppbv gaseous pinonaldehyde. Pinonaldehyde yields from the photochemical degradation of α-pinene with OH were measured in laboratory experiments ranging from 6 to 87 % (Larsen et al., 2001; Noziére et al., 1999). The high variability could be due to different chemical conditions with partly high reactant concentrations used in these experiments. A recent study in the atmospheric simulation chamber SAPHIR used ambient reactant concentrations ([α-pinene] $\leq$ 3.8 ppbv, [NO] < 120 pptv, (310 ± 5) K) and reported a low yield of 5 % (Rolletter et al., 2019). As currently implemented in the Master Chemical Mechanism (MCM, 2017; Jenkin et al., 1997; Saunders et al., 2003) pinonaldehyde is formed with a total yield of 84 %. In contrast, a theory based study by Vereecken et al. (2007) suggested a different branching ratio of initial RO_2 and additional reaction channels which lead in total to pinonaldehyde yields of 60 % for low atmospheric NO conditions ($\leq$ 1 ppbv NO). Our previous study (Rolletter et al., 2019) showed that further adjustment of the initial RO_2 branching ratio in a mechanism based

on Vereecken et al. (2007) was necessary to explain the low measured pinonaldehyde yield of 5 % for conditions similar to the experiments discussed here. A similar change in RO_2 branching ratios was found in an experimental study by Xu et al. (2019)~.

The photochemistry of pinonaldehyde has been investigated in only few experimental studies (Noziére et al., 1999; Jaoui and Kamens, 2003; Capouet et al., 2004) in addition to few theoretical studies (Glasius et al., 1997; Vereecken and Peeters, 2002; Fantechi et al., 2002; Dash and Rajakumar, 2012). The pinonaldehyde degradation during daytime is controlled by photolysis and the reaction with OH radicals resulting in an atmospheric lifetime on the order of a few hours due to its fast reaction with OH (Atkinson et al., 2004). The lifetime of pinonaldehyde with respect to photodissociation strongly depends on the season and the latitude, but can be comparable to the reaction with OH (Hallquist et al., 1997). Main oxidation products (Fig. 1) of the photolysis and OH reactions are norpinonaldehyde (NORPINAL; names are taken from the MCM), pinonic acid (PINONIC), perpinonic acid (PERPINONIC), formaldehyde (HCHO), and acetone. So far, there has been only one study by Noziére et al. (1999) reporting yields for the reaction with OH for HCHO and acetone of (152 ± 56) % and (15 ± 7) %, respectively.

A simplified oxidation scheme of pinonaldehyde is shown in Fig. 1. As implemented in the ~~Master Chemical Mechanism (MCM, 2017; Jenkin et al., 1997; Saunders et al., 2003)~~MCM, the photolysis of pinonaldehyde (PINAL) leads to dissociation in HCO and an organic radical, both of which react with O_2 to form CO, HO_2 and the peroxy radical C96O2.

$$PINAL + h\nu + O_2 \quad \rightarrow \quad C96O2 + CO + HO_2 \tag{R1}$$

The oxidation of pinonaldehyde by OH is initiated by H-abstraction mainly at the aldehyde group forming primary ~~peroxy radicals (~~RO_2~~)~~. In the MCM, an acyl peroxy radical (C96CO3) and PINALO2 are formed.

$$PINAL + OH + O_2 \quad \rightarrow \quad C96CO3 \quad (\text{yield} : 0.77) \tag{R2}$$
$$PINAL + OH + O_2 \quad \rightarrow \quad PINALO2 \quad (\text{yield} : 0.23) \tag{R3}$$

In the presence of high nitric oxide (NO) concentrations, RO_2 react with NO and form either alkoxy radicals (RO) or organic nitrate compounds ($RONO_2$). In the reaction forming an alkoxy radical, NO is converted to NO_2 and HO_2 to OH, respectively. The alkoxy radical subsequently reacts with O_2 to form a carbonyl compound and HO_2, decomposes or isomerizes. At low NO concentrations, RO_2 reactions with HO_2 terminating the radical chain reactions and forming stable hydroxyperoxides (ROOH) gain in importance. Formed stable organic products of $RO_2 + NO$ and $RO_2 + HO_2$ reactions can further react with OH or photolyse.

The reaction of the most important RO_2 radical, C96CO3 with HO_2 can either directly form the same product (C96O2) as its reaction with NO or can form the stable products pinonic and perpinonic acid. Subsequently, pinonic and perpinonic acid are photolyzed or react with OH and thereby producing again the peroxy radical C96O2. Similarly, other $RO_2 + HO_2$ reactions not shown in Fig. 1 produce the same species which are produced by $RO_2 + NO$ reactions.

In the atmosphere, the peroxy radical C96O2 can react with nitric oxide (NO) to form the corresponding alkoxy radical C96O.

$$C96O2 + NO \quad \rightarrow \quad C96O + NO_2 \tag{R4}$$

C96O undergoes isomerization or decomposition reactions producing formaldehyde, acetone or 3,4-dioxopentanal (CO23C4CHO).

The main products of the subsequent chemistry of the other peroxy radical PINALO2, including multiple reactions with NO and decomposition reactions, are HO_2, a tri-carbonyl compound, acetone, and formaldehyde.

5   In contrast to the MCM, the theoretical study by Fantechi et al. (2002) predicts other decomposition reactions of products of the $RO_2 + NO$ reaction (Fig. 1). Whereas other theory based studies investigated the reaction rate of pinonaldehyde $+ OH$ (Glasius et al., 1997) and the probability of H-abstraction by OH at various sites of pinonaldehyde (Vereecken and Peeters, 2002; Dash and Rajakumar, 2012), Fantechi et al. (2002) analysed also the subsequent chemistry of the initially formed organic peroxy radicals. Instead of forming acetone and formaldehyde in the further degradation of C96O, Fantechi et al. (2002)

10 suggest that the the main fraction of C96O undergoes a series of isomerization reactions and reactions with NO forming 4-hydroxynorpinonaldehyde. In contrast to the MCM, the four-membered ring structure is retained in the formed products. A small fraction (~ 7%) directly forms norpinonaldehyde (NORPINAL) after H-abstraction by O_2. The modifications by Fantechi et al. (2002) are limited to $RO_2 + NO$ chemistry and no detailed analysis of $RO_2 + HO_2$ reactions was done in their work. Nevertheless, modifications suggested by Fantechi et al. (2002) also affect $RO_2 + HO_2$ chemistry, if products from these

15 reactions are the same as from the reaction of $RO_2 + NO$ as implemented in the MCM. In the model by Fantechi et al. (2002) some $RO_2 + NO$ reactions also lead to the formation of organic nitrates with yields between 14 % and 28 %, which lower the yield of formed HO_2 and carbonyl compounds.

    Fantechi et al. (2002) proposed two additional relevant (yields > 5 %) peroxy radicals formed by the initial OH attack. Accordingly, the yields of C96CO3 and PINALO2 are changed from 77 % to 61 % and 23 % to 9 % compared to the MCM,

20 respectively. The first additional reaction channel with a branching ratio of 24 % leads to a formation of norpinonaldehyde. The second additional reaction channel with only a minor contribution of 6 % forms in the subsequent chemistry acetone, formaldehyde and a tri-carbonyl-hydroxy compound.

    In this work, the photochemistry of pinonaldehyde was investigated under controlled, atmospheric conditions including atmospherically reactant concentrations and natural sunlight in the outdoor chamber SAPHIR (Simulation of Atmospheric

25 PHotochemistry In a large Reaction Chamber) at Forschungszentrum Jülich. This study focusses on (a) the determination of the pinonaldehyde photolysis frequency, (b) quantification of HO_x $(= OH + HO_2)$ radicals in the OH–oxidation of pinonaldehyde, and (c) the determination of acetone and formaldehyde yields of both photolysis and OH–oxidation. Measurements of pinonaldehyde, degradation products and HO_X radicals are compared to model calculations applying the Master Chemical Mechanism v3.3.1. Sensitivity model runs are performed including reaction pathways and yields suggested by the theoretical

30 study of Fantechi et al. (2002) and the impact of the proposed mechanism on concentrations of organic compounds and HO_x $(= OH +)$ radicals is analyzed.

2 Methods

2.1 Atmospheric simulation chamber SAPHIR

Details of the SAPHIR chamber can be found elsewhere (e.g. Rohrer et al., 2005; Bohn et al., 2005) and the chamber is only briefly described here. It is of cylindrical shape (18 m length, 5 m diameter, and 270 m^3 volume) and is made of a double wall FEP film. The FEP ensures inertness of the surfaces and minimizes wall effects. This outdoor chamber allows studying the photochemical reactions under natural sunlight, because the FEP film is transmissive for the entire solar spectrum. The chamber is equipped with a shutter system that can shield the chamber from sunlight.

Ultra-pure synthetic air used in the experiments is mixed from liquid nitrogen and oxygen (Linde, purity >99.9999 %). The pressure inside the chamber is slightly (30 Pa) above ambient pressure to prevent impurities from ambient air leaking into the chamber. Air that is consumed by instruments or is lost due to small leakages is replenished to keep a constant pressure. The replenishment flow is in the range of 9 to 12 m^{3}h^{-1} leading to a dilution of trace gases of 3 to 4 % h^{-1}. Rapid mixing of air is ensured by the operation of two fans inside the chamber.

In the sunlit chamber, there are small sources for nitrous acid (HONO), formaldehyde (HCHO), and acetone. Their formation rates depend on the intensity of solar radiation, relative humidity and temperature (Rohrer et al., 2005). The photolysis of HONO is the major primary source for nitrogen oxides and OH. Approximately, 250 pptv h^{-1} NO$_x$, 200 pptv h^{-1} HCHO and 100 pptv h^{-1} acetone were formed in the experiments in this study.

2.2 Instrumentation

An overview of used instruments and their 1 σ accuracies and precision is given in Table 1.

OH radicals were measured by laser induced fluorescence (LIF). The instrument operated at the SAPHIR chamber has been described elsewhere (e.g. Holland et al., 2003; Fuchs et al., 2012). Chamber air is sampled through an inlet nozzle into a low-pressure measurement cell, where OH is excited by pulsed laser radiation at 308 nm. Its fluorescence is subsequently detected by gated photon counting. In addition, HO$_2$ radicals are indirectly detected after chemical conversion to OH by NO in another measurement cell (Fuchs et al., 2011). The instrument is calibrated by a radical source, in which OH and HO$_2$ are produced by water vapor photolysis at 185 nm (Fuchs et al., 2011).

Interferences can occur in the HO$_2$ measurements because of concurrent conversion of specific RO$_2$ radicals which produce OH in the reaction with NO on a similar time scale as HO$_2$ does (Fuchs et al., 2011; Whalley et al., 2013; Lew et al., 2018). Because the conversion of RO$_2$ requires at least two reaction steps with NO in contrast to HO$_2$ for which only one reaction step leads to the formation of OH, this interference can be minimized, if the conversion efficiency of HO$_2$ is below 10 %. This can be achieved by adjusting the NO concentration in the HO$_2$ cell. This was done in this study, so that it can be assumed that potential interferences in the HO$_2$ detection were negligible.

In addition, OH was measured by differential optical absorption spectrometry (DOAS; Dorn et al., 1995b) which is an absolute measurement technique. Measured OH concentrations of both instruments agreed on average within 15 % similar to results in previous experiments (Fuchs et al., 2012).

Organic compounds were measured by proton transfer reaction time-of-flight mass spectrometry (PTR-TOF-MS; Lindinger et al., 1998; Jordan et al., 2009) and by gas chromatography that was coupled to a flame ionization detector (GC-FID). Formaldehyde was measured by a Hantzsch instrument and by DOAS.

Photolysis frequencies (j) of NO_2, HONO, O_3, and pinonaldehyde were calculated from actinic flux density spectra that are derived from measurements of total and diffuse spectral actinic flux densities outside the chamber~~:~~

$$j = \int \sigma(\lambda)\phi(\lambda)F_\lambda(\lambda)\mathrm{d}\lambda$$

~~with σ the absorption cross section, ϕ the quantum yield, and F the actinic flux~~. From these measurements direct sun contributions are calculated. The direct and diffuse actinic flux densities are ~~then~~ used as input for a model which calculates mean chamber spectra by taking into account the time-dependent effects of shadings of the chamber steel frame and the transmittance of the Teflon ~~films (Bohn and Zilken, 2005). The method is regularly evaluated by dedicated experiments using the chamber as a chemical actinometer (Bohn et al., 2005)~~ film which is > 0.8 in the complete solar spectral range (Bohn and Zilken, 2005). Mean photolysis frequencies are then calculated by the following equation:

$$j = \int \sigma(\lambda)\phi(\lambda)F_\lambda(\lambda)\mathrm{d}\lambda \tag{1}$$

with σ the absorption cross section, ϕ the quantum yield, and F the actinic flux. The absorption ~~spectra~~ cross sections and quantum yields ~~used for the calculations~~ of NO_2, HONO, and O_3 ~~to calculate~~ used for the calculations of photolysis frequencies are taken from the literature (Mérienne et al., 1995; Troe, 2000; Stutz et al., 2000; Daumont et al., 1992; Matsumi et al., 2002). The method is regularly evaluated by dedicated experiments using the chamber as a chemical actinometer (Bohn et al., 2005). The pinonaldehyde photolysis frequency is discussed in more detail in Section 4.1.

NO and NO_2 were measured by chemiluminescence (Eco Physics), water vapor mixing ratios by a cavity ring-down instrument (Picarro) and ozone (O_3) by an UV absorption instrument (Ansyco).

2.3 Experimental procedure

Before the experiment, the chamber was flushed with dry, synthetic air to dilute trace gases from previous experiments below the detection limits of the instruments. Twenty ppm of CO_2 was injected as a dilution tracer in the beginning of each experiment. Water from a Milli-Q-device was boiled and flushed into the chamber together with a high flow of synthetic air ($150\,\mathrm{m^3 h^{-1}}$). The chamber was only humidified in the beginning of an experiment reaching initial water vapor concentrations of about 2 % which decreased over the course of an experiment due to the dilution with dry synthetic air.

Pinonaldehyde (Orgentis chemicals, 98.2 %) was heated in a glass vial and the vapor was flushed together with a small flow of dry nitrogen into the chamber using a short Teflon tube. After the injection had been stopped, the sample line was removed to avoid further evaporation of pinonaldehyde from the injection system into the chamber. The initial pinonaldehyde concentrations were 6.5 and 16.5 ppbv in the experiments on 17 July and 18 July 2014, respectively. The chamber roof was opened after a stable pinonaldehyde concentration was observed by the PTR-TOF-MS instrument.

In one experiment (18 July 2014), 2500 ppbv of cyclohexane was additionally injected after the humidification. Cyclohexane served as scavenger for OH in this experiment in order to study the pinonaldehyde photolysis independently from its reaction with OH.

In the other experiment (17 July 2014), 70 ppbv of ozone produced from a silent discharge ozonizer (O3Onia) was injected after humidification, so that a low NO concentration (maximum 80 pptv) was obtained during the experiment. In this experiment, approximately 20 % of reacted pinonaldehyde was photolyzed and the remaining 80 % reacted with OH. The reaction of pinonaldehyde with ozone is very slow (k = (8.9 ± 1.4) x 10^{-20}cm^{3}s^{-1}, Glasius et al. (1997)) and therefore ozonolysis reactions did not play a role in the experiments here.

2.4 Model calculations

The Master Chemical Mechanism (MCM) in its latest version 3.3.1 was applied as base model for box model calculations (MCM, 2017; Jenkin et al., 1997; Saunders et al., 2003). FACSIMILE was used as solver for differential equations in the model calculations.

In order to account for chamber effects, the following modifications were added to the MCM model. Dilution to all trace gases was applied. The dilution rate was calculated from the monitored replenishment flow rate that was consistent with the ~~diluton~~ dilution of the CO_2 tracer. Small chamber sources of formaldehyde and acetone were parameterized based on reference experiments as described in Rohrer et al. (2005); Karl et al. (2006); Kaminski et al. (2017).

Temperature, pressure, H_2O, NO, NO_2, HONO, and O_3 concentrations were constrained to measured values. These constrains were used because chamber NO sources cannot be modeled accurately and therefore could lead to wrong conclusions in the analysis of turnover rates of radicals.

Photolysis frequencies, which were not measured, were calculated for clear sky conditions by the parameterization included in the MCM. They were scaled to take cloud cover and the transmission of the Teflon film into account by the ratio of measured to modeled photolysis frequency of NO_2. This applies also for the photolysis frequency of pinonaldehyde in the base model case (MCM). All other model runs used the experimentally derived pinonaldehyde photolysis frequency (see Section 4.1).

The injection of pinonaldehyde was modeled as a source only present during the time period of injection to match the pinonaldehyde increase as measured by PTR-TOF-MS.

In a sensitivity study, the pinonaldehyde oxidation scheme developed by Fantechi et al. (2002) was implemented. In this mechanism, additional reaction pathways of the pinonaldehyde reaction with OH that are not included in the MCM are suggested. Only the four reaction pathways with significant yields (> 5 %) were implemented for the sensitivity model run (Fig. 1). In addition, the fate of the most abundant RO_2 formed from the reaction of pinonaldehyde with OH or photolysis is different in this model compared to the MCM mechanism (see above). Reaction rate constants and branching ratios were used as described in Fantechi et al. (2002). Simple rate coefficients such as KDEC (= 1 x 10^6) and KRO2NO (= 2.7 x 10^{-12} exp(360/T)) from the MCM were used, when no specific reaction rate constants were mentioned. To account for possible $RO_2 + HO_2$ reactions, a reaction scheme based on the reaction C97O2 + HO_2 was added for all newly introduced RO_2 species not included in the MCM. $RO_2 + HO_2$ reactions form a corresponding hydroxyperoxide (ROOH) that can either react with OH to regenerate the RO_2

or photolyse to form the corresponding alkoxy radical (RO). Modifications by Fantechi et al. (2002) describe the chemistry from the OH attack on pinonaldehyde until the formation of stable products 4-hydroxynorpinonaldehyde, norpinonaldehyde, CO23C4CHO, and C818CO. The chemistry of the products norpinonaldehyde, CO23C4CHO and C818CO was treated as described in the MCM. For 4-hydroxynorpinonaldehyde, no follow-up chemistry was considered.

5 Both MCM and Fantechi et al. (2002) mechanism were tested under different conditions. An overview of used model calulations is given in Table 2.

3 Results

Figures 2 and 3 show the concentration time series of pinonaldehyde and other measured trace gases together with MCM model results for the two experiments with and without OH scavenger, respectively.

10 Weather conditions were similar for both experiment days. The temperature inside the chamber increased over the course of each experiment from 305 to 315 K. The solar zenith angle at noon was 30 $^\circ$ and maximum measured pinonaldehyde photolysis frequencies were approximately 3.5×10^{-5} s^{-1} in both experiments.

In both experiments, the measured pinonaldehyde decay was significantly faster than predicted by the model once the chamber roof was opened. The predicted pinonaldehyde consumption rate was slower by 50 % and 25 % in the pure photolysis

15 case and in the OH oxidation case, respectively. Potential wall loss of pinonaldehyde in the chamber was tested in separate experiments, in which pinonaldehyde was injected into the dark chamber. The loss of pinonaldehyde in this case is consistent with the dilution calculated from the replenishment flow.

Also the two measured major organic products, acetone and formaldehyde, are not well reproduced by the model calculations. In the experiment with the OH scavenger, in which pinonaldehyde is removed by photolysis only, the modeled concentra-

20 tions of formaldehyde and acetone are 60 % and 70 % higher compared to the measurements, although the photolysis frequency of pinonaldehyde is obviously underestimated. In contrast, in the experiment in which pinonaldehyde was photolyzed and oxidized by OH modeled acetone concentrations are underestimated by 17 % compared to measurements. Modeled formaldehyde concentrations are 6 % smaller than measurements, which is within the measurement uncertainty. The smaller modeled acetone yield cannot be explained only by the lower consumption of pinonaldehyde in the model. A sensitivity run which reproduces

25 the pinonaldehyde consumption also underestimates the acetone concentrations.

In the experiment without scavenger, OH and HO$_2$ are both considerably underpredicted by the MCM. While OH shows an increasing discrepancy of up to a factor of 2, modeled HO$_2$ is a factor of 2–4 lower than measured. In the experiment with OH scavenger, measured and modeled HO$_2$ concentrations agree within the stated uncertainty during the first part of the experiment, but the model underestimates the HO$_2$ by 50 % in the last hour.

30 Measured time series of acetone and formaldehyde are used to determine the total yields of acetone and formaldehyde from the pinonaldehyde oxidation following the procedure described by Galloway et al. (2011), Kaminski et al. (2017), and Rolletter et al. (2019). In this approach, the measured time series of trace gases are corrected for loss and production that are not directly related to the chemical oxidation scheme of pinonaldehyde. This includes dilution of trace gases in the chamber, loss

of formaldehyde due to photolysis and small production of formaldehyde and acetone in the sunlit chamber that is independent from the pinonaldehyde chemistry. If also OH is present, additional corrections for the losses of formaldehyde and acetone due to their reactions with OH are applied. The corrected time series can then be used to calculate the ratio of a formed organic product and the consumed pinonaldehyde to derive the yield of the organic compound that is connected to the chemical degradation of pinonaldehyde. The main uncertainty in the calculated yields is caused by the uncertainty of the strength of the small chamber sources which has to be taken from characterization experiments that were performed before/after the experiments with pinonaldehyde. Sensitivity studies in which the source strengths are systematically varied show that 1σ uncertainties of yields are 0.2 and 0.1 for formaldehyde and acetone, respectively.

Figure 4 shows the result of the yield calculations. The formaldehyde yield is (0.1 ± 0.2) in the beginning and increases to approximately (0.18 ± 0.2) in the end of the experiment. The acetone yield of the photolysis is zero within the uncertainty of 0.1.

The yields of acetone and formaldehyde are also calculated from the measured time series in the experiment when pinonaldehyde was oxidized by OH as described for the experiment with OH scavenger. Results are shown in Fig. 5. The yields of both species increase over the course of the experiment. The formaldehyde yield increases from approximately (0.15 ± 0.2) to values higher than (0.45 ± 0.2) and the acetone yield from approximately (0.2 ± 0.1) to (0.3 ± 0.1).

4 Discussion

4.1 Pinonaldehyde photolysis

In the presence of an OH scavenger, the pinonaldehyde decay observed in the chamber could be due to photolysis, wall loss and dilution. As was shown by additional experiments in the dark chamber, wall loss is negligible on the time scale of a few hours. The effect of dilution was quantified from the measured dilution flow rate and the chamber volume and agreed with the results from the tracer (CO_2) measurements within 3 %. Without OH, the chemical degradation of pinonaldehyde depends only on the photolysis frequency of pinonaldehyde. In MCM, photolysis frequencies are generally calculated as a function of solar zenith angle χ using three parameters l, m, and n.

$$J = l \cdot (\cos(\chi))^m \cdot e^{(-n \cdot \sec(\chi))} \tag{2}$$

For pinonaldehyde, MCM is using the parameters ($l = 2.792 \times 10^{-5} s^{-1}$, m = 0.805, n = 0.338; valid for clear sky conditions) for the photolysis of n-butanal. The parameterization is based on the absorption spectrum measured for n-butanal at 298 K by Martinez et al. (1992) and the quantum yield (0.21) for its dissociation to n-C_3H_7 + HCO at 298 K and 1 atm by Tadić et al. (2001). For the evaluation of the chamber experiments, the clear sky values from the parameterization (Equation 1) are corrected for the influence of cloud cover and chamber transmission by multiplying the clear sky value by the ratio of the measured to parametrized photolysis frequency of NO_2. Following this procedure, the simulated decay of pinonaldehyde in the base model (MCM) is considerably slower than the observed decay (Fig. 6).

As an alternative, the photolysis frequency of pinonaldehyde is calculated using the measured spectrally-resolved solar actinic flux (Section 2.2) and the pinonaldehyde absorption spectrum (280-340 nm) measured at 300 K by Hallquist et al. (1997). Good agreement between the observed and simulated (MCM_a) pinonaldehyde decay is achieved, if an effective quantum yield of 0.9 is assumed (Fig. 6, upper panel). Here, the mean decay rate of pinonaldehyde between 10:00 and 15:00 (UTC)

5 is $3.9 \times 10^{-5}\,\mathrm{s}^{-1}$, of which $2.9 \times 10^{-5}\,\mathrm{s}^{-1}$ is caused by photolysis and $1.0 \times 10^{-5}\,\mathrm{s}^{-1}$ by dilution. The experimentally derived photolysis frequencies are approximately a factor of 3 to 3.5 higher than the values from the parameterization in the MCM. The experimental error (20 %) of the effective quantum yield (0.9) is mainly determined by the uncertainties of the absorption spectrum (< 5 %; Hallquist et al. (1997)) and the actinic flux measurement (10 %). Error contributions from wall loss and dilution are small (< 5 %).

10 The applied absorption cross sections by Hallquist et al. (1997) are the only published measurements and are recommended by IUPAC (Atkinson et al., 2006). The effective, wavelength-independent quantum yield determined in this work is significantly higher than in two other chamber studies, which report values of 0.14 ± 0.03 (Moortgat et al., 2002) and 0.4 (Jaoui and Kamens, 2003) for photolysis with natural sunlight. No recommendation for the quantum yield is given by IUPAC (Atkinson et al., 2006). Both chamber studies applied the absorption spectrum from Hallquist et al. (1997) for the calculation of photolysis

15 frequencies. Jaoui and Kamens (2003) measured the solar radiation by a UV-Eppley radiometer. The broadband instrument measures the spectrally integrated solar irradiance (spatially cosine-weighted photon-flux density) from 300 nm to 400 nm. The non-trivial conversion to a actinic flux spectrum (spatially isotropically weighted photon-flux density) between 300 nm and 340 nm needed for the evaluation of the pinonaldehyde photoloysis frequencies has not been documented by the authors. The conversion requires knowledge of the spatial distribution of the incident solar radiation, which is a function of solar zenith

20 angle, wavelength, atmospheric aerosol and clouds (Hofzumahaus, 2006). Furthermore, the wavelength range of pinonaldehyde photolysis (< 340 nm) strongly depends on the total atmospheric ozone column, while UV Eppley measurements (300-400 nm) are only weakly dependent on total ozone. Considerable errors may therefore be connected to the conversion of Eppley data to photolysis frequencies for pinonaldehyde.

In the study by Moortgat et al. (2002), solar actinic flux was directly measured by a spectroradiometer with good accuracy

25 like in the present work. However, similar to Jaoui and Kamens (2003), Moortgat et al. (2002) had to apply large corrections for wall losses and dilution, each of which were of the same magnitude as the photolysis rate. The large difference by a factor of 7 in comparison to the present work is likely not explained by systematic errors of the correction.

The pinonaldehyde photolysis is faster than n-butanal because of its two carbonyl functions. This might be valid for other bi-carbonyl compounds that have non-conjugated carbonyl functions, so that the use of the n-butanal photolysis frequency

30 could systematically underestimate the photolysis frequencies of these compounds. However, the high quantum yield close to unity could also be a specific property of pinonaldehyde that might not apply for the photolysis of other bi-carbonyl species.

Figure 4 shows the time series of measured acetone and formaldehyde concentrations together with results from model calculations applying the MCM. In contrast to the base case model (MCM, Fig. 2), measured photolysis frequencies are used (MCM_a). As a consequence of the the higher photolysis frequencies, the consumption of pinonaldehyde leads to even larger

productions of formaldehyde and acetone (approximately three times higher than measured values) compared to the base case model.

For conditions of this experiment, 80 % of RO_2 radicals formed in the photolysis reaction of pinonaldehyde are reacting with NO and only 20 % are reacting with HO_2, so that carbonyl compounds are expected to be the main organic products (Fig. 1). Acetone measured in this experiment is solely formed by the chamber source. Initial acetone yield values are negative because of the high uncertainty in the corrections that are applied in the yield calculation. In the beginning of an experiment, only small amounts of products are formed which leads to a large uncertainty, so that negative values are not significant. It has to be stressed here again that the parametrization of the chamber source is the main uncertainty in the yield calculation. If the chamber source was overestimated, the constant measured acetone yield could also include a small contribution from the pinonaldehyde photolysis.

In a sensitivity model run (FAN_a), the pinonaldehyde oxidation scheme suggested by Fantechi et al. (2002) is tested for the experiment with OH scavenger. While the initial photodissociation step and the reaction of C96O2 with NO are the same, the following decomposition of C96O yields considerably different organic products. No acetone and less formaldehyde are produced together with mainly 4-hydroxynorpinonaldehyde and norpinonaldehyde that were not measured in these experiments. Agreement between modeled and measured acetone is achieved within the accuracy of measurements of 10 %. Also modeled formaldehyde concentrations are only 20 % lower than measured values. Thus, the model description of acetone and formaldehyde products is greatly improved by the use of the Fantechi et al. (2002) mechanism compared to the MCM.

To our knowledge, there is only one other study by Jaoui and Kamens (2003), which investigated the product yields of pinonaldehyde photolysis. Products were measured by gas-chromatography in that chamber study in the presence and absence of an OH scavenger. The measured norpinonaldehyde yield agrees within the stated uncertainty with the yield proposed by Fantechi et al. (2002). Formaldehyde and acetone yields were not measured by Jaoui and Kamens (2003).

Using the MCM with the measured photolysis frequency (MCM_a) leads to an increase in modeled HO_2 of about 25 % (Fig. 6, lower panel) which can be explained by the higher amount of consumed pinonaldehyde that is formed at the end of the radical reaction chain together with 3,4-dioxopentanal (CO23C4CHO). Unfortunately, between 11:30 and 14:00 experimental problems occurred in the HO_2 measurements. Neither NO measurements nor photolysis frequencies showed any features that could explain the decrease in the HO_2 concentration. The exact reason of the HO_2 variations remains unclear and the uncertainty of HO_2 measurements is likely higher (50 %) for this period. Implementing the modifications by Fantechi et al. (2002) results in a HO_2 concentration time profile (FAN_a) that is different from both model runs done with the MCM mechanism. In the FAN_a model run HO_2 is formed more rapidly compared to the MCM and concentrations decrease towards the end of the experiment. The rate determining step in radical chain reactions is the reaction of RO_2 with NO forming an alkoxy radical and NO_2. In the MCM, there are 3 $RO_2 + NO$ reactions before the radical chain is terminated and the stable product CO23C4CHO is formed together with HO_2. In contrast, in the Fantechi et al. (2002) mechanism only one $RO_2 + NO$ reaction occurs before the stable products are formed and HO_2 is regenerated. In addition, no subsequent chemistry of the formed product 4-hydroxynorpinonaldehyde is included in the model which would produce additional HO_2, especially in later stages of the experiment.

4.2 Photooxidation by OH

In the photooxidation experiment without OH scavenger (Fig. 2~~3~~), a much faster decay of pinonaldehyde is observed compared to the case with OH scavenger (Fig. ~~3~~2). Without scavenger, 30 % of the decay in the beginning of the experiment is explained by photolysis and 5 % by dilution. The remaining 65 % are due to the removal of pinonaldehyde by OH. However, OH concentrations ~~raise~~ rise over the course of the experiment and the pinonaldehyde fraction reacting with OH increase to up to 80 %. Here and in the following analysis, experimental photolysis frequencies are used, which assume a quantum yield of 0.9 (see Section 4.1). The photolysis and the OH reaction of pinonaldehyde lead to a mix of peroxy radicals (Fig. 1), which react mainly with HO_2 or NO. During the experiment, the NO mixing ratio increases from about 10 pptv to 80 pptv. Accordingly, the fraction of RO_2 radicals reacting with NO increases from 20 % to 55 %, while the RO_2 fraction reacting with HO_2 decreases.

Applying the experimental pinonaldehyde photolysis frequency to the model (MCM_a) improves the simulation of the pinonaldehyde decay compared to the base model run (MCM), which uses a slower parameterized photolysis frequency. However, even with the faster photolysis rate, the consumption of pinonaldehyde is underestimated (Fig. 7, upper panel). At the end of the experiment (15:00), the remaining modeled pinonaldehyde concentration is a factor of 2 larger than the measured value. This is due to the lower OH concentration in the model compared to measurements. If modeled OH concentrations are increased to match measured values, which can be achieved by constraining HO_2 in the model to measurements (MCM_b), modeled and measured pinonaldehyde concentrations agree within 10 % (Fig. 7~~, lower panel~~). This demonstrates that missing OH production in the model is most likely due to the underestimation of HO_2, which forms OH by reaction with NO. This suggests that there is a HO_2 source missing in the model. In a sensitivity run (not shown here) artificial HO_2 sources were added to the model to quantify the required HO_2 source strength. The missing HO_2 source is increasing over the course of the experiment. A source strength between $0.8\,\mathrm{ppbv\,h^{-1}}$ and $1.5\,\mathrm{ppbv\,h^{-1}}$ would be required to explain observations. The consumption of pinonaldehyde during the experiment is up to $2.5\,\mathrm{ppbv\,h^{-1}}$, so that a comparably large HO_2 source would be required.

Implementation of the mechanism by Fantechi et al. (2002) does not improve the model-measurement agreement of OH and HO_2 (Fig. 8) compared to the MCM. As discussed above, the mechanism by Fantechi et al. (2002) is able to describe HO_2 concentrations as well as product formation of acetone and HCHO, if pinonaldehyde is only consumed by photolysis. In contrast, reaction pathways that are connected to the reaction of pinonaldehyde + OH are not correctly described.

Modeled HO_2 concentrations could be affected by the use of general reaction rate constants for reactions of RO_2 with HO_2 and NO (KRO2HO2 and KRO2NO), respectively. This might be an oversimplification for highly functionalized compounds. A sensitivity test (see Supplement) with an enhanced reaction rate for $RO_2 + NO$ reactions of $2\times$ KRO2NO in the modified mechanism by Fantechi et al. (2002) was performed. As a result, the fraction of RO_2 reacting with NO instead of HO_2 is increased. This leads to an enhanced HO_2 concentration of approximately 50 % compared to the model run FAN_a. However, HO_x concentrations are again underestimated compared to measurements and the sensitivity run cannot reproduce the HO_2 concentration time behaviour from observations.

Besides reactions with NO, new types of RO_2 reactions have been recognized in the last decade that can produce HO_x. These processes include unimolecular autoxidation reactions of RO_2 (e.g. Crounse et al., 2013) and reactions of RO_2 with HO_2 yielding OH (e.g. Hasson et al., 2004). The new types of reactions become potentially important, when NO concentrations are below 1 ppbv. These reactions are especially favoured when the RO_2 molecule contains functional groups, like carbonyl

5   groups as in the case of pinonaldehyde peroxy radicals. For example, acetyl- and acetonyl-RO_2 can react with HO_2 forming alkoxy radicals and OH instead of terminating the radical reaction chain forming hydroxyperoxides (Hasson et al., 2004; Dillon and Crowley, 2008). Other examples are reactions already included in the MCM~~like found in~~, such as the photooxidation of methyl vinyl ketone (Praske et al., 2015; Fuchs et al., 2018). For pinonaldehyde, there have been no comparable reactions suggested so far, although pinonaldehyde and its degradation products have at least 2 carbonyl functions. Because 80 to 45 %

10   of RO_2 reacts with HO_2 for conditions of the experiment here, such reaction pathways have the potential to impact the OH production rate. A sensitivity test (not shown here) shows that $RO_2 + HO_2$ reactions of RO_2 included in the mechanism with a rate of $10\times$ KRO2HO2 can reproduce measured OH concentrations. Nevertheless, the enhanced HO_2 consumption increases the model-measurement discrepancy of HO_2 even more.

Reported autoxidation reactions of RO_2, which produce HO_x without NO, involve isomerization and decomposition of

15   organic peroxy radicals. These reactions play a role, for example, in the photooxidation of isoprene (e.g. Fuchs et al., 2013; Peeters et al., 2014; Novelli et al., 2020) and methacrolein (Crounse et al., 2012; Fuchs et al., 2014), where H-shift reactions in RO_2 species lead to decomposition into a radical (OH or HO_2) and a carbonyl compound. In general, rate coefficients of H-shift reactions are strongly enhanced by the presence of functional groups such as carbonyl groups, and can reach values in the order of 0.1 s^{-1} at room temperature (Crounse et al., 2013; Otkjær et al., 2018). Depending on the specific RO_2 structure

20   and its functional groups, either OH or HO_2 can be formed. The presence of hydroxyl or hydroperoxy groups in carbonyl peroxy radicals, for example, favours the elimination of HO_2.

In the chemical degradation of pinonaldehyde to its first-generation products (Fig. 1), a large number of multifunctional peroxy and alkoxy radicals are formed as intermediates. Thus, there is potential for additional HO_2 formation by unimolecular reactions. This possibility is explored in a model sensitivity run for the four oxidation branches I - IV (Fantechi et al., 2002),

25   which follow OH addition to pinonaldehyde. The model run S1 (~~Table 2~~see Supplement) assumes that each of the initially formed peroxy radicals (C96CO3, FAN_D1, PINALO2, and FAN_G1) is eventually converted to HO_2 with a rate coefficient of 0.1 s^{-1}. However, only FAN_D1, PINALO2, and FAN_G1 have an aldehyde group with a hydrogen that can be easily abstracted (see Supplementary material). The model run (Fig. 8) shows a considerable enhancement of the HO_2 concentration level in the first period of the experiment compared to model runs MCM_a and FAN_a, leading to good agreement between

30   modeled and measured OH. However, the temporal trend of the modeled HO_2 is not well described. While the observed HO_2 shows a steady increase from the beginning to the end of the experiment, the simulation S1 shows a continuous decrease which follows the concentration of the short-lived RO_2 radicals. The opposite temporal trend suggests that additional HO_2 formation by a fast process in the oxidation branches I - IV is not a likely explanation. It indicates that the additionally required HO_2 is slowly built up, probably from stable products of the pinonaldehyde oxidation.

One such possibility would be the photolysis of first-generation products. This idea is tested in model run S2 (Table 2, Fig. 8). All products of the pinonaldehyde photooxidation have either two or three carbonyl groups and therefore are likely to undergo photolysis. CO23C4CHO and C818CO even have conjugated carbonyl functions similar to glyoxal, which photolysis is up to two times faster than pinonaldehyde. However, using the photolysis frequency of glyoxal as an upper limit for the photolysis

5 frequency of the products formed here, is not sufficient to significantly improve the HO_2 model-measurement agreement. Only if a strongly enhanced photolysis frequency equivalent to $0.2 \times j_{NO2}$ is applied, modeled HO_2 comes close to the observed values. In this case, the temporal trend of the simulation is similar to the observed time behaviour of HO_2 and also OH is reasonably well reproduced. This supports the hypothesis that the additional HO_2 is slowly formed from stable oxidation products. However, the value for the assumed photolysis frequency, which is 200 times larger than of pinonaldehyde, appears

10 unrealistically high. ~~Further research of possible mechanisms by theoretical and experimental techniques will be needed to explain the unknown~~

Another possibility is that the fast H-shift isomerization of RO_2 radicals (see Supplement) leads to the formation of peroxy acids with additional carbonyl functions in high yields. As discussed above, these bi-functional compounds could photolyse faster than currently implemented in the mechanism. A sensitivity test (S1_mod_hv, see Supplement) was performed that

15 includes isomerization of RO_2 with a –HCO group. Products are assumed to photolyse with a photolysis rate that is 2 times higher than that of glyoxal. Implementation of these reactions leads to HO_2 ~~source~~concentrations that are increased by up to 60 % compared to the sensitivity run that includes only isomerization reactions. Calculated HO_2 concentrations underestimate measurements by factor of 2. The sensitivity test reproduces measured OH concentrations within the measurement uncertainty.

No subsequent chemistry of 4-hydroxynorpinonaldehyde is included in the mechanism so far. In the experiment here

20 4-hydroxynorpinonaldehyde is formed with an overall yield of approximately 25 %. 4-hydroxynorpinonaldehyde is highly functionalized and RO_2 radicals formed in its degradation could undergo fast isomerization reactions. For a sensitivity run (S3, see Supplement) a mechanism was deduced with the structure–activity relationship (SAR; Kwok and Atkinson, 1995; Vereecken and Peeter method. However, the impact of the tested 4-hydroxynorpinonaldehyde degradation scheme on the HO_2 formation was small (≤ 10 %) compared to the modified mechanism by Fantechi et al. (2002). Unfortunately, no measurements of stable oxidation

25 products other than acetone and HCHO were available. Without further product measurements the whole analysis discussed here relies on product distribution prescribed by the models. Further experiments that measure oxidation products and yields could help to better constrain branching ratios in degradation mechanisms. In addition, theoretical studies could investigate subsequent degradation schemes of major products in more detail.

The continuous increase in the acetone and formaldehyde yields during the experiment (Fig. 5) indicates that both species

30 are not only formed from the first reaction step of pinonaldehyde with OH, but also from further oxidation of organic products.

The base model (Fig. 3, MCM) underestimates the pinonaldehyde consumption, but shows a good model-measurement agreement with formaldehyde and acetone within the measurement uncertainty. In contrast, the model, which uses measured pinonaldehyde photolysis frequencies and is constrained to measured HO_2, produces up to 30 % less acetone and formaldehyde than measured (Fig. 5, MCM_b). The discrepancies are increasing fast during the first 2 hours of the experiment, when

35 pinonaldehyde is the most important reaction partner for OH, and slows down, when oxidation products gain importance at

15

later times of the experiment. The elevated HO_2 concentrations change the product distribution compared to the base case with less formed formaldehyde and acetone, because $RO_2 + HO_2$ reactions producing hydroxyperoxides become more important compared to the $RO_2 + NO$ pathway. In the chemical model, acetone and formaldehyde of this reaction pathway are formed by the slow photolysis (10 times slower than the photolysis of pinonaldehyde) of pinonic acid and perpinonic acid that are produced in the subsequent chemistry of hydroxyperoxides. Therefore, acetone and formaldehyde yields are smaller in the MCM model run, if HO_2 concentrations are correctly described compared to the base case MCM model, when HO_2 is significantly underestimated.

Implementation of the mechanism by Fantechi et al. (2002) with also HO_2 concentrations and pinonaldehyde photolysis frequency constrained to measurements (FAN_b) makes the model-measurement agreement for acetone and formaldehyde worse. Acetone and formaldehyde yields are lowered and 4-hydroxynorpinonaldehyde and norpinonaldehyde are produced instead. Acetone and formaldehyde time series agree for the photolysis experiment, when the mechanism by Fantechi et al. (2002) is applied. Similarly, the majority of consumed pinonaldehyde (approximately 65 %) forms the peroxy radical C96O2 either by photolysis or reaction pathway I (Fig. 1), when also OH is present. Therefore, it can be assumed that the C96O2 + NO reaction channel is not responsible for the underprediction of acetone and formaldehyde at least for the early times of the experiments, when contributions from OH reactions of product species are small. However, because $RO_2 + HO_2$ reactions are more important in the experiment with OH oxidation (see above), additional HO_2 production from this reaction pathway has the potential to serve as an explanation for the observed disccrepancies. In addition, minor pathways could produce additional formaldehyde and acetone to explain the model-measurement discrepancy right after the start of the pinonaldehyde oxidation. At later times of the experiment, additional production of acetone and formaldehyde from the further degradation of oxidation products need to be assumed to close the gap. For example, this could be due to a reaction channel of the alkoxy radical $R'O8$ that does not produce norpinonaldehyde, but acetone and formaldehyde instead. However, the exact chemical mechanism that is responsible for the additional acetone and formaldehyde cannot be determined from measurements in these experiments.

Presently, there is only one work of Noziére et al. (1999) where acetone and formaldehyde were quantitatively measured for the reaction of pinonaldehyde with OH. The formaldehyde yield was determined to be 1.52 ± 0.56, significantly higher than the yield measured in this work. The acetone yield in Noziére et al. (1999) lies with 0.15 ± 0.07 in the range of the acetone yield determined here for the times of the experiment when pinonaldehyde is the dominant OH reactant. In the oxidation scheme of pinonaldehyde acetone and formaldehyde are typically formed together so that similar yields would be expected. The high HCHO yield measured by Noziére et al. (1999) can be partially explained by additional fast photolysis of pinonaldehyde and possibly other products by the $254\,nm$ lamps used to generate OH by photodissociaton of H_2O_2 (Fantechi et al., 2002).

5 Summary and conclusions

The photooxidation of pinonaldehyde was investigated under natural sunlight at low NO concentrations (< 0.2 ppbv) in the presence and absence of an OH scavenger. Two experiments were conducted with maximum pinonaldehyde concentrations

of 16.5 ppbv (with OH scavenger) and 6.5 ppbv (without OH scavenger). Measured times series were compared to model calculations based on the recent version of the Master Chemical Mechanism (version ~~3.1~~3.3.1).

Model results show that the pinonaldehyde consumption is underestimated in the experiment with OH scavenger. In contrast, the concentration of the measured products acetone and formaldehyde is overestimated by 60 % and 70 %, respectively. The observed decay of pinonaldehyde requires a quantum yield of 0.9 for the photolysis reaction. Previous investigations of the quantum yield determined lower yields of 0.15 (Moortgat et al., 2002) and ≤ 0.4 (Jaoui and Kamens, 2003). However, the solar actinic flux could not accurately be determined in these other chamber studies and large corrections for wall loss were applied. Calculations using the measured absorption spectrum (Hallquist et al., 1997) and a quantum yield of 0.9 give photolysis frequencies, which are a factor of 3.5 times higher than values calculated by the parameterization implemented in the MCM, so that photolysis of pinonaldehyde is significantly underestimated, if this parameterization is applied.

Similarly, the pinonaldehyde consumption is underestimated by the MCM model in the experiment, where the pinonaldehyde consumption is dominated by its reaction with OH radicals. Implementing the measured photolysis frequency improves model-measurement agreement. The remaining discrepancy is caused by underestimated OH radical concentrations leading to a slower pinonaldehyde consumption. Constraining HO_2 model concentrations to the measurements brings OH concentrations in model and measurement into agreement. As a consequence, also the pinonaldehyde concentration profile is reproduced within the measurement uncertainty. The closed OH budget indicates that a HO_2 source is missing in this mechanism. The additional HO_2 source would be at least half the rate at which pinonaldehyde is consumed. HO_2 would therefore need to be reproduced much faster than current chemical models suggest in one of the major oxidation pathways. Because a large fraction of RO_2 radicals (45-80 %) react with HO_2, potential reaction pathways that do not lead to the formation of hydroxyperoxide but reform radicals have the potential to contribute the regeneration of HO_2. If fast uni-molecular RO_2 reactions existed that could compete with $RO_2 + NO$ and $RO_2 + HO_2$ reactions, they could also add to additional HO_2 production. Nevertheless, a fast degradation of first-generation products species forming HO_2 shows a better agreement with measured HO_2 concentration time profiles rather than reactions of RO_2 species.

The yield of formaldehyde in the pinonaldehyde photolysis with OH scavenger present is determined to be 0.18 ± 0.20. No acetone formation is observed. Model calculations based on the MCM constrained with the measured photolysis frequency overestimate formaldehyde and acetone concentrations by a factor of approximately 3. In the experiment with OH the yields of acetone and formaldehyde increase over the course of the experiment from (0.2 ± 0.1) to (0.3 ± 0.1) and from (0.15 ± 0.2) to (0.45 ± 0.2) respectively. The increasing yields indicate that both species are also formed by the subsequent chemistry of products formed in the first reaction steps.

Modifications of the degradation mechanism proposed by Fantechi et al. (2002), including a new product distribution and additional products for the initial attack of OH, reproduce measured acetone and formaldehyde concentrations within their uncertainty as long as the reaction with OH is supressed. In the experiment with OH, the model-measurement agreement for both species decrease after implementing the modifications by Fantechi et al. (2002). This indicates that the pathways relevant when OH is dominating the fate of pinonaldehyde lack sources of acetone and formaldehyde in this case.

Field campaigns in environments dominated by monoterpene emissions like the Bio-hydro-atmosphere interactions of Energy, Aerosols, Carbon, H2O, Organics, and Nitrogen–Rocky Mountain Organic Carbon Study (BEACHON-ROCS; Kim et al., 2013) or the Hyytiälä United Measurements of Photochemistry and Particles in Air — Comprehensive Organic Precursor Emission and Concentration study (HUMPPA-COPEC; Hens et al., 2014) showed that OH and HO_2 radical concentrations were underestimated in model calculations by up to a factor of 2.5. Constraining modeled HO_2 concentrations to measurements allowed reproducing OH radical concentrations. In addition, also chamber studies on the photooxidation of α-pinene (Rolletter et al., 2019) and β-pinene (Kaminski et al., 2017) confirmed that the current α and β-pinene mechanisms lack HO_2 sources. It is currently unknown, if the missing source is part of reactions forming first generation products or of the subsequent chemistry of the degradation products. Here, it is shown that also in the mechanism of the photoxodidation of pinonaldehyde, a degradation product of α-pinene, a HO_2 source is missing. However, the findings here cannot explain the discrepancies observed in the α-pinene chamber experiments and field campaigns, because the pinonaldehyde yield in the α-pinene degradation is rather small (5 %, Rolletter et al. (2019)). Nevertheless, this result is an example for a second-generation species that produces significantly more HO_2 than suggested in current chemical models. Further ~~investigations~~ experiments will be required to investigate, if also other oxidation products from the degradation of monoterpenes could explain observations of missing HO_2 sources.

Author contributions. MR analysed the data and wrote the paper. HF and MK designed the experiments. HF conducted the HO_x radical measurements. BB conducted the radiation measurements. MK and RW were responsible for the GC measurements. RT was responsible for the PTR-TOF-MS measurements. XL was responsible for the HONO measurements and HPD for the DOAS OH data. FR was responsible for the NO_x and O_3 data. All co-authors commented on the manuscript.

Competing interests. The authors declare to have no competing interests.

References

Alves, C., Carvalho, A., and Pio, C.: Mass balance of organic carbon fractions in atmospheric aerosols, J. Geophys. Res. Atmos., 107, ICC 7–1–ICC 7–9, https://doi.org/10.1029/2001jd000616, 2002.

Atkinson, R. and Arey, J.: Atmospheric degradation of volatile organic compounds, Chem. Rev., 103, 4605–4638, https://doi.org/10.1021/cr0206420, 2003.

Atkinson, R., Baulch, D. L., Cox, R. A., Crowley, J. N., Hampson, R. F., Hynes, R. G., Jenkin, M. E., Rossi, M. J., and Troe, J.: Evaluated kinetic and photochemical data for atmospheric chemistry: Volume I - gas phase reactions of O_x, HO_x, NO_x and SO_x species, Atmos. Chem. Phys., 4, 1461–1738, https://doi.org/10.5194/acp-4-1461-2004, 2004.

Atkinson, R., Baulch, D. L., Cox, R. A., Crowley, J. N., Hampson, R. F., Hynes, R. G., Jenkin, M. E., Rossi, M. J., Troe, J., and Subcommittee, I.: Evaluated kinetic and photochemical data for atmospheric chemistry: Volume II - gas phase reactions of organic species, Atmos. Chem. Phys., 6, 3625–4055, https://doi.org/10.5194/acp-6-3625-2006, 2006.

Bohn, B. and Zilken, H.: Model-aided radiometric determination of photolysis frequencies in a sunlit atmosphere simulation chamber, Atmos. Chem. Phys., 5, 191–206, https://doi.org/10.5194/acp-5-191-2005, 2005.

Bohn, B., Rohrer, F., Brauers, T., and Wahner, A.: Actinometric measurements of NO_2 photolysis frequencies in the atmosphere simulation chamber SAPHIR, Atmos. Chem. Phys., 5, 493–503, https://doi.org/10.5194/acp-5-493-2005, 2005.

Boy, M., Petäjä, T., Dal Maso, M., Rannik, U., Rinne, J., Aalto, P., Laaksonen, A., Vaattovaara, P., Joutsensaari, J., Hoffmann, T., Warnke, J., Apostolaki, M., Stephanou, E. G., Tsapakis, M., Kouvarakis, A., Pio, C., Carvalho, A., Römpp, A., Moortgat, G., Spirig, C., Guenther, A., Greenberg, J., Ciccioli, P., and Kulmala, M.: Overview of the field measurement campaign in Hyytiälä, August 2001 in the framework of the EU project OSOA, Atmos. Chem. Phys., 4, 657–678, https://doi.org/10.5194/acp-4-657-2004, 2004.

Cahill, T. M., Seaman, V. Y., Charles, M. J., Holzinger, R., and Goldstein, A. H.: Secondary organic aerosols formed from oxidation of biogenic volatile organic compounds in the Sierra Nevada Mountains of California, J. Geophys. Res. Atmos., 111, 14, https://doi.org/10.1029/2006jd007178, 2006.

Calogirou, A., Larsen, B. R., and Kotzias, D.: Gas-phase terpene oxidation products: a review, Atmos. Environ., 33, 1423–1439, https://doi.org/10.1016/S1352-2310(98)00277-5, 1999.

Capouet, M., Peeters, J., Noziére, B., and Müller, J. F.: Alpha-pinene oxidation by OH: simulations of laboratory experiments, Atmos. Chem. Phys., 4, 2285–2311, https://doi.org/10.5194/acp-4-2285-2004, 2004.

Crounse, J. D., Knap, H. C., Ornso, K. B., Jorgensen, S., Paulot, F., Kjaergaard, H. G., and Wennberg, P. O.: On the atmospheric fate of methacrolein: 1. Peroxy radical isomerization following addition of OH and O_2, J. Phys. Chem. A, 116, 5756–5762, https://doi.org/10.1021/jp211560u, 2012.

Crounse, J. D., Nielsen, L. B., Jørgensen, S., Kjaergaard, H. G., and Wennberg, P. O.: Autoxidation of organic compounds in the atmosphere, J. Phys. Chem. Lett., 4, 3513–3520, https://doi.org/10.1021/jz4019207, 2013.

Dash, M. R. and Rajakumar, B.: Abstraction kinetics of H-atom by OH radical from pinonaldehyde ($C_{10}H_{16}O_2$): Ab initio and transition-state theory Calculations, J. Phys. Chem. A, 116, 5856–5866, https://doi.org/10.1021/jp209208e, 2012.

Daumont, D., Brion, J., Charbonnier, J., and Malicet, J.: Ozone UV spectroscopy I: Absorption cross-sections at room temperature, J. Atmos. Chem., 15, 145–155, https://doi.org/10.1007/bf00053756, 1992.

Dillon, T. J. and Crowley, J. N.: Direct detection of OH formation in the reactions of HO_2 with $CH_3C(O)O_2$ and other substituted peroxy radicals, Atmos. Chem. Phys., 8, 4877–4889, https://doi.org/10.5194/acp-8-4877-2008, 2008.

Dorn, H.-P., Brandenburger, U., Brauers, T., and Hausmann, M.: A new in-situ laser long-path absorption instrument for the measurement of tropospheric OH radicals, J. Atmos. Sci., 52, 3373–3380, 1995a.

Dorn, H. P., Neuroth, R., and Hofzumahaus, A.: Investigation of OH absorption cross sections of rotational transitions in the $A^2\Sigma^+, \nu' = 0 \leftarrow X^2\Pi, \nu'' = 0$ band under atmospheric conditions: Implications for tropospheric long-path absorption measurements, J. Geophys. Res., 100, 7397–7409, https://doi.org/10.1029/94jd03323, 1995b.

Eurochamp: Database of Atmospheric Simulation Chamber Studies, https://data.eurochamp.org/, last access: 9 September, 2019.

Fantechi, G., Vereecken, L., and Peeters, J.: The OH-initiated atmospheric oxidation of pinonaldehyde: Detailed theoretical study and mechanism construction, Phys. Chem. Chem. Phys., 4, 5795–5805, https://doi.org/10.1039/B205901K, 2002.

Fuchs, H., Bohn, B., Hofzumahaus, A., Holland, F., Lu, K. D., Nehr, S., Rohrer, F., and Wahner, A.: Detection of HO_2 by laser-induced fluorescence: calibration and interferences from RO_2 radicals, Atmos. Meas. Tech., 4, 1209–1255, https://doi.org/10.5194/amt-4-1209-2011, 2011.

Fuchs, H., Dorn, H. P., Bachner, M., Bohn, B., Brauers, T., Gomm, S., Hofzumahaus, A., Holland, F., Nehr, S., Rohrer, F., Tillmann, R., and Wahner, A.: Comparison of OH concentration measurements by DOAS and LIF during SAPHIR chamber experiments at high OH reactivity and low NO concentration, Atmos. Meas. Tech., 5, 1611–1626, https://doi.org/10.5194/amt-5-1611-2012, 2012.

Fuchs, H., Hofzumahaus, A., Rohrer, F., Bohn, B., Brauers, T., Dorn, H.-P., Häseler, R., Holland, F., Kaminski, M., Li, X., Lu, K., Nehr, S., Tillmann, R., Wegener, R., and Wahner, A.: Experimental evidence for efficient hydroxyl radical regeneration in isoprene oxidation, Nat. Geosci., 6, 1023–1026, https://doi.org/10.1038/NGEO1964, 2013.

Fuchs, H., Acir, I. H., Bohn, B., Brauers, T., Dorn, H. P., Häseler, R., Hofzumahaus, A., Holland, F., Kaminski, M., Li, X., Lu, K., Lutz, A., Nehr, S., Rohrer, F., Tillmann, R., Wegener, R., and Wahner, A.: OH regeneration from methacrolein oxidation investigated in the atmosphere simulation chamber SAPHIR, Atmos. Chem. Phys., 14, 7895–7908, https://doi.org/10.5194/acp-14-7895-2014, 2014.

Fuchs, H., Albrecht, S., Acir, I. H., Bohn, B., Breitenlechner, M., Dorn, H. P., Gkatzelis, G. I., Hofzumahaus, A., Holland, F., Kaminski, M., Keutsch, F. N., Novelli, A., Reimer, D., Rohrer, F., Tillmann, R., Vereecken, L., Wegener, R., Zaytsev, A., Kiendler-Scharr, A., and Wahner, A.: Investigation of the oxidation of methyl vinyl ketone (MVK) by OH radicals in the atmospheric simulation chamber SAPHIR, Atmos. Chem. Phys., 2018, 8001–8016, https://doi.org/10.5194/acp-18-8001-2018, 2018.

Galloway, M. M., Huisman, A. J., Yee, L. D., Chan, A. W. H., Loza, C. L., Seinfeld, J. H., and Keutsch, F. N.: Yields of oxidized volatile organic compounds during the OH radical initiated oxidation of isoprene, methyl vinyl ketone, and methacrolein under high-NO_X conditions, Atmos. Chem. Phys., 11, 10 779–10 790, https://doi.org/10.5194/acp-11-10779-2011, 2011.

Glasius, M., Calogirou, A., Jensen, J., Hjorth, J., and Nielsen, C. J.: Kinetic study of gas-phase reactions of pinonaldehyde and structurally related compounds, Int. J. Chem. Kin., 29, 527–533, https://doi.org/10.1002/(sici)1097-4601(1997)29:7<527::Aid-kin7>3.0.Co;2-w, 1997.

Guenther, A. B., Jiang, X., Heald, C. L., Sakulyanontvittaya, T., Duhl, T., Emmons, L. K., and Wang, X.: The model of emissions of gases and aerosols from nature version 2.1 (MEGAN2.1): an extended and updated framework for modeling biogenic emissions, Geosci. Model Dev., 5, 1471–1492, https://doi.org/10.5194/gmd-5-1471-2012, 2012.

Hallquist, M., Wängberg, I., and Ljungström, E.: Atmospheric fate of carbonyl oxidation products originating from α-pinene and Δ^3-carene: determination of rate of reaction with OH and NO_3 radicals, UV absorption cross sections, and vapor pressures, Environ. Sci. Technol., 31, 3166–3172, https://doi.org/10.1021/es970151a, 1997.

Hasson, A. S., Tyndall, G. S., and Orlando, J. J.: A product yield study of the reaction of HO_2 radicals with ethyl peroxy ($C_2H_5O_2$), acetyl peroxy ($CH_3C(O)O_2$), and acetonyl peroxy ($CH_3C(O)CH_2O_2$) radicals, J. Phys. Chem. A, 108, 5979–5989, https://doi.org/10.1021/jp048873t, 2004.

Hausmann, M., Brandenburger, U., Brauers, T., and Dorn, H.-P.: Detection of tropospheric OH radicals by long-path differential-optical-absorption spectroscopy: Experimental setup, accuracy, and precision, J. Geophys. Res., 102, 16 011–16 022, https://doi.org/10.1029/97jd00931, 1997.

Hens, K., Novelli, A., Martinez, M., Auld, J., Axinte, R., Bohn, B., Fischer, H., Keronen, P., Kubistin, D., Nölscher, A. C., Oswald, R., Paasonen, P., Petäjä, T., Regelin, E., Sander, R., Sinha, V., Sipilä, M., Taraborrelli, D., Tatum Ernest, C., Williams, J., Lelieveld, J., and Harder, H.: Observation and modelling of HO_X radicals in a boreal forest, Atmos. Chem. Phys., 14, 8723–8747, https://doi.org/10.5194/acp-14-8723-2014, 2014.

Herckes, P., Engling, G., Kreidenweis, S. M., and Collett, J. L.: Particle size distributions of organic aerosol constituents during the 2002 Yosemite Aerosol Characterization Study, Environ. Sci. Technol., 40, 4554–4562, https://doi.org/10.1021/es0515396, 2006.

Hofzumahaus, A.: Measurement of Photolysis Frequencies in the Atmosphere, in: Analytical Techniques for Atmospheric Measurement, D.E. Heard (Ed.), book section 9, pp. 406–500, https://doi.org/10.1002/9780470988510.ch9, 2006.

Holland, F., Hofzumahaus, A., Schäfer, J., Kraus, A., and Pätz, H. W.: Measurements of OH and HO_2 radical concentrations and photolysis frequencies during BERLIOZ, J. Geophys. Res., 108, 8246, https://doi.org/10.1029/2001JD001393, 2003.

Jacob, D. J., Field, B. D., Jin, E. M., Bey, I., Li, Q., Logan, J. A., and Yantosca, R. M.: Atmospheric acetone budget, J. Geophys. Res., 107, 4100, https://doi.org/10.1029/2001JD000694, 2002.

Jaoui, M. and Kamens, R. M.: Gas phase photolysis of pinonaldehyde in the presence of sunlight, Atmos. Environ., 37, 1835–1851, https://doi.org/10.1016/S1352-2310(03)00033-5, 2003.

Jenkin, M. E., Saunders, S. M., and Pilling, M. J.: The tropospheric degradation of volatile organic compounds: A protocol for mechanism development, Atmos. Environ., 31, 81–104, https://doi.org/10.1016/S1352-2310(96)00105-7, 1997.

Jordan, A., Haidacher, S., Hanel, G., Hartungen, E., Märk, L., Seehauser, H., Schottkowsky, R., Sulzer, P., and Märk, T. D.: A high resolution and high sensitivity proton-transfer-reaction time-of-flight mass spectrometer (PTR-TOF-MS), Int. J. Mass Spectrom., 286, 122–128, https://doi.org/10.1016/j.ijms.2009.07.005, 2009.

Kaminski, M., Fuchs, H., Acir, I. H., Bohn, B., Brauers, T., Dorn, H. P., Häseler, R., Hofzumahaus, A., Li, X., Lutz, A., Nehr, S., Rohrer, F., Tillmann, R., Vereecken, L., Wegener, R., and Wahner, A.: Investigation of the β-pinene photooxidation by OH in the atmosphere simulation chamber SAPHIR, Atmos. Chem. Phys., 17, 6631–6650, https://doi.org/10.5194/acp-17-6631-2017, 2017.

Kanakidou, M., Tsigaridis, K., Dentener, F. J., and Crutzen, P. J.: Human-activity-enhanced formation of organic aerosols by biogenic hydrocarbon oxidation, J. Geophys. Res., 105, 9243–9354, https://doi.org/10.1029/1999JD901148, 2000.

Karl, M., Dorn, H.-P., Holland, F., Koppmann, R., Poppe, D., Rupp, L., Schaub, A., and Wahner, A.: Product study of the reaction of OH radicals with isoprene in the atmosphere simulation chamber SAPHIR, J. Atmos. Chem., 55, 167–187, https://doi.org/10.1007/s10874-006-9034-x, 2006.

Kavouras, I. G., Mihalopoulos, N., and Stephanou, E. G.: Formation and gas/particle partitioning of monoterpenes photo-oxidation products over forests, Geophys. Res. Lett., 26, 55–58, https://doi.org/10.1029/1998gl900251, 1999.

Kim, S., Wolfe, G. M., Mauldin, L., Cantrell, C., Guenther, A., Karl, T., Turnipseed, A., Greenberg, J., Hall, S. R., Ullmann, K., Apel, E., Hornbrook, R., Kajii, Y., Nakashima, Y., Keutsch, F. N., DiGangi, J. P., Henry, S. B., Kaser, L., Schnitzhofer, R., Graus, M., and Hansel, A.: Evaluation of HO_X sources and cycling using measurement-constrained model calculations in a 2-methyl-3-butene-2-ol (MBO) and monoterpene (MT) dominated ecosystem, Atmos. Chem. Phys., 13, 2031–2044, https://doi.org/10.5194/acp-13-2031-2013, 2013.

Kwok, E. S. C. and Atkinson, R.: Estimation of hydroxyl radical reaction rate constants for gas-phase organic compounds using a structure-reactivity relationship: An update, Atmos. Environ., 29, 1685–1695, https://doi.org/10.1016/1352-2310(95)00069-B, 1995.

Larsen, B. R., Di Bella, D., Glasius, M., Winterhalter, R., Jensen, N. R., and Hjorth, J.: Gas-phase OH oxidation of monoterpenes: Gaseous and particulate products, J. Atmos. Chem., 38, 231–276, https://doi.org/10.1023/A:1006487530903, 2001.

Lew, M. M., Dusanter, S., and Stevens, P. S.: Measurement of interferences associated with the detection of the hydroperoxy radical in the atmosphere using laser-induced fluorescence, Atmos. Meas. Tech., 11, 95–108, https://doi.org/10.5194/amt-11-95-2018, 2018.

5   Li, X., Rohrer, F., Hofzumahaus, A., Brauers, T., Häseler, R., Bohn, B., Broch, S., Fuchs, H., Gomm, S., Holland, F., Jäger, J., Kaiser, J., Keutsch, F. N., Lohse, I., Lu, K., Tillmann, R., Wegener, R., Wolfe, G. M., Mentel, T. F., Kiendler-Scharr, A., and Wahner, A.: Missing gas-phase source of HONO inferred from Zeppelin measurements in the troposphere, Science, 344, 292–296, https://doi.org/10.1126/science.1248999, 2014.

Lindinger, W., Hansel, A., and Jordan, A.: On-line monitoring of volatile organic compounds at pptv levels by means of proton-transfer-reaction mass spectrometry (PTR-MS) - Medical applications, food control and environmental research, Int. J. Mass Spectrom., 173, 191–241, https://doi.org/10.1016/s0168-1176(97)00281-4, 1998.

Martinez, R. D., Buitrago, A. A., Howell, N. W., Hearn, C. H., and Joens, J. A.: The near U.V. absorption spectra of several aliphatic aldehydes and ketones at 300 K, Atmos. Environ., 26, 785–792, https://doi.org/10.1016/0960-1686(92)90238-G, 1992.

Matsumi, Y., Comes, F. J., Hancock, G., Hofzumahaus, A., Hynes, A. J., Kawasaki, M., and Ravishankara, A. R.: Quantum yields for production of O(^{1}D) in the ultraviolet photolysis of ozone: Recommendation based on evaluation of laboratory data, J. Geophys. Res. Atmos., 107, ACH 1–1–ACH 1–12, https://doi.org/10.1029/2001jd000510, 2002.

MCM: Master Chemical Mechanism, http://mcm.leeds.ac.uk/MCM/, last access: 04 March 2020, 2017.

Mérienne, M. F., Jenouvrier, A., and Coquart, B.: The NO_2 absorption spectrum. I: Absorption cross-sections at ambient temperature in the 300-500 nm region, J. Atmos. Chem., 20, 281–297, https://doi.org/10.1007/bf00694498, 1995.

20 Moortgat, G., Wirtz, K., Hjorth, J., Ljungstrom, E., Ruppert, L., Hayman, G., and Mellouki, W.: 'Evaluation of radical sources in atmospheric chemistry through chamber and laboratory studies', Final report on the EU project 'RADICAL', Report EUR 20254 EN., 2002.

Müller, K., Haferkorn, S., Grabmer, W., Wisthaler, A., Hansel, A., Kreuzwieser, J., Cojocariu, C., Rennenberg, H., and Herrmann, H.: Biogenic carbonyl compounds within and above a coniferous forest in Germany, Atmos. Environ., 40, 81–91, https://doi.org/10.1016/j.atmosenv.2005.10.070, 2006.

25 Novelli, A., Vereecken, L., Bohn, B., Dorn, H. P., Gkatzelis, G. I., Hofzumahaus, A., Holland, F., Reimer, D., Rohrer, F., Rosanka, S., Taraborrelli, D., Tillmann, R., Wegener, R., Yu, Z., Kiendler-Scharr, A., Wahner, A., and Fuchs, H.: Importance of isomerization reactions for OH radical regeneration from the photo-oxidation of isoprene investigated in the atmospheric simulation chamber SAPHIR, Atmos. Chem. Phys., 20, 3333–3355, https://doi.org/10.5194/acp-20-3333-2020, 2020.

Noziére, B., Barnes, I., and Becker, K.-H.: Product study and mechanisms of the reactions of α-pinene and of pinonaldehyde with OH radicals, J. Geophys. Res., 104, 23 645–23 656, https://doi.org/10.1029/1999JD900778, 1999.

30 Otkjær, R. V., Jakobsen, H. H., Tram, C. M., and Kjaergaard, H. G.: Calculated Hydrogen Shift Rate Constants in Substituted Alkyl Peroxy Radicals, J. Phys. Chem. A,, 122, 8665–8673, https://doi.org/10.1021/acs.jpca.8b06223, 2018.

Peeters, J., Vereecken, L., and Fantechi, G.: The detailed mechanism of the OH-initiated atmospheric oxidation of α-pinene: a theoretical study, Phys. Chem. Chem. Phys., 3, 5489–5504, https://doi.org/10.1039/B106555F, 2001.

35 Peeters, J., Müller, J.-F., Stavrakou, T., and Nguyen, V. S.: Hydroxyl radical recycling in isoprene oxidation driven by hydrogen bonding and hydrogen tunneling: The upgraded LIM1 mechanism, J. Phys. Chem. A, 118, 8625–8643, https://doi.org/10.1021/jp5033146, 2014.

Plewka, A., Gnauk, T., Bruggemann, E., and Herrmann, H.: Biogenic contributions to the chemical composition of airborne particles in a coniferous forest in Germany, Atmos. Environ., 40, S103–S115, https://doi.org/10.1016/j.atmosenv.2005.09.090, 2006.

Praske, E., Crounse, J. D., Bates, K. H., Kurten, T., Kjaergaard, H. G., and Wennberg, P. O.: Atmospheric fate of methyl vinyl ketone: Peroxy radical reactions with NO and HO_2, J. Phys. Chem. A, 119, 4562–4572, https://doi.org/10.1021/jp5107058, 2015.

Rissanen, T., Hyotylainen, T., Kallio, M., Kronholm, J., Kulmala, M., and Rikkola, M. L.: Characterization of organic compounds in aerosol particles from a coniferous forest by GC-MS, Chemosphere, 64, 1185–1195, https://doi.org/10.1016/j.chemosphere.2005.11.079, 2006.

5 Rohrer, F. and Brüning, D.: Surface NO and NO_2 mixing ratios measured between $30°N$ and $30°S$ in the Atlantic region, J. Atmos. Chem., 15, 253–267, https://doi.org/10.1029/97JD01853, 1992.

Rohrer, F., Bohn, B., Brauers, T., Brüning, D., Johnen, F.-J., Wahner, A., and Kleffmann, J.: Characterisation of the photolytic HONO-source in the atmosphere simulation chamber SAPHIR, Atmos. Chem. Phys., 5, 2189–2201, https://doi.org/10.5194/acp-5-2189-2005, 2005.

Rolletter, M., Kaminski, M., Acir, I. H., Bohn, B., Dorn, H. P., Li, X., Lutz, A., Nehr, S., Rohrer, F., Tillmann, R., Wegener, R., Hofzumahaus,
10 A., Kiendler-Scharr, A., Wahner, A., and Fuchs, H.: Investigation of the α-pinene photooxidation by OH in the atmospheric simulation chamber SAPHIR, Atmos. Chem. Phys., 19, 11 635–11 649, https://doi.org/10.5194/acp-19-11635-2019, 2019.

Satsumabayashi, H., Nishizawa, H., Yokouchi, Y., and Ueda, H.: Pinonaldehyde and some other organics in rain and snow in central Japan, Chemosphere, 45, 887–891, https://doi.org/10.1016/s0045-6535(01)00024-8, 2001.

Saunders, S. M., Jenkin, M. E., Derwent, R. G., and Pilling, M. J.: Protocol for the development of the Master Chemical Mecha-
15 nism, MCMv3 (Part A): Tropospheric degradation of non-aromatic volatile organic compounds, Atmos. Chem. Phys., 3, 161–180, https://doi.org/10.5194/acp-3-161-2003, 2003.

Schlosser, E., Bohn, B., Brauers, T., Dorn, H.-P., Fuchs, H., Häseler, R., Hofzumahaus, A., Holland, F., Rohrer, F., Rupp, L. O., Siese, M., Tillmann, R., and Wahner, A.: Intercomparison of two hydroxyl radical measurement techniques at the atmosphere simulation chamber SAPHIR, J. Atmos. Chem., 56, 187–205, https://doi.org/10.1007/s10874-006-9049-3, 2007.

20 Schwantes, R. H., Emmons, L. K., Orlando, J. J., Barth, M. C., Tyndall, G. S., Hall, S. R., Ullmann, K., St. Clair, J. M., Blake, D. R., Wisthaler, A., and Bui, T. P. V.: Comprehensive isoprene and terpene gas-phase chemistry improves simulated surface ozone in the southeastern US, Atmos. Chem. Phys., 20, 3739–3776, https://doi.org/10.5194/acp-20-3739-2020, 2020.

Stutz, J., Kim, E. S., Platt, U., Bruno, P., Perrino, C., and Febo, A.: UV-visible absorption cross sections of nitrous acid, J. Geophys. Res. Atmos., 105, 14 585–14 592, https://doi.org/10.1029/2000jd900003, 2000.

25 Tadić, J., Juranić, I., and Moortgat, G. K.: Pressure dependence of the photooxidation of selected carbonyl compounds in air: n-butanal and n-pentanal, J. Photochem. Photobiol. A, 143, 169–179, https://doi.org/https://doi.org/10.1016/S1010-6030(01)00524-X, 2001.

Troe, J.: Are primary quantum yields of NO2 photolysis at $\lambda \leq 398$ nm smaller than unity?, Z. Phys. Chem., 214, 573, https://doi.org/10.1524/zpch.2000.214.5.573, 2000.

Vereecken, L. and Nozière, B.: H migration in peroxy radicals under atmospheric conditions, Atmos. Chem. Phys., 20, 7429–7458,
30 https://doi.org/10.5194/acp-20-7429-2020, 2020.

Vereecken, L. and Peeters, J.: Enhanced H-atom abstraction from pinonaldehyde, pinonic acid, pinic acid, and related compounds: theoretical study of C-H bond strengths, Phys. Chem. Chem. Phys., 4, 467–472, https://doi.org/10.1039/B109370C, 2002.

Vereecken, L. and Peeters, J.: Decomposition of substituted alkoxy radicals-part I: a generalized structure-activity relationship for reaction barrier heights, Phys. Chem. Chem. Phys., 11, 9062–9074, https://doi.org/10.1039/B909712K, 2009.

35 Vereecken, L., Müller, J. F., and Peeters, J.: Low-volatility poly-oxygenates in the OH-initiated atmospheric oxidation of α-pinene: impact of non-traditional peroxyl radical chemistry, Phys. Chem. Chem. Phys., 9, 5241–5248, https://doi.org/10.1039/B708023A, 2007.

Whalley, L. K., Blitz, M. A., Desservettaz, M., Seakins, P. W., and Heard, D. E.: Reporting the sensitivity of laser-induced fluorescence instruments used for HO_2 detection to an interference from RO_2 radicals and introducing a novel approach that enables HO_2 and certain RO_2 types to be selectively measured, Atmos. Meas. Tech., 6, 3425–3440, https://doi.org/10.5194/amt-6-3425-2013, 2013.

Xu, L., Møller, K. H., Crounse, J. D., Otkjær, R. V., Kjaergaard, H. G., and Wennberg, P. O.: Unimolecular Reactions of Peroxy Radicals Formed in the Oxidation of α-Pinene and β-Pinene by Hydroxyl Radicals, J. Phys. Chem. A,, 123, 1661–1674, https://doi.org/10.1021/acs.jpca.8b11726, 2019.

Yu, J. Z., Griffin, R. J., Cocker, D. R., Flagan, R. C., Seinfeld, J. H., and Blanchard, P.: Observation of gaseous and particulate products of monoterpene oxidation in forest atmospheres, Geophys. Res. Lett., 26, 1145–1148, https://doi.org/10.1029/1999gl900169, 1999.

Table 1. Instrumentation for radical and trace gas detection during the pinonaldehyde oxidation experiments.

	Technique	Time Resolution	1σ Precision	1σ Accuracy
OH	DOAS[a] (Dorn et al., 1995a; Hausmann et al., 1997; Schlosser et al., 2007)	205 s	0.8×10^6 cm^{-3}	6.5 %
OH	LIF[b] (Holland et al., 2003; Fuchs et al., 2012)	47 s	0.3×10^6 cm^{-3}	13 %
HO$_2$	LIF[b] (Fuchs et al., 2011)	47 s	1.5×10^7 cm^{-3}	16 %
NO	Chemiluminescence (Rohrer and Brüning, 1992)	180 s	4 pptv	5 %
NO$_2$	Chemiluminescence (Rohrer and Brüning, 1992)	180 s	2 pptv	5 %
O$_3$	UV absorption (Ansyco)	10 s	5 ppbv	5 %
pinonaldehyde, acetone	PTR-TOF-MS[c] (Lindinger et al., 1998)	30 s	15 pptv	6 %
acetone	GC-FID[d] (Kaminski et al., 2017)	30 min	20 pptv	5 %
HCHO	Hantzsch monitor (AeroLaser)	120 s	20 pptv	5 %
HCHO	DOAS[a]	100 s	20 %	10 %
HONO	LOPAP[e] (Li et al., 2014)	300 s	1.3 pptv	13 %
Photolysis frequencies	Spectroradiometer (Bohn et al., 2005)	60 s	10 %	10 %

[a] Differential Optical Absorption Spectroscopy

[b] Laser Induced Fluorescence

[c] Proton-Transfer-Reaction Time-Of-Flight Mass-Spectrometry

[d] Gas Chromatography Flame-Ionization-Detector

[e] Long-Path-Absorption-Photometer

Table 2. Overview of different model calculations.

Model run	Model	$j_{pinonaldehyde}$	HO_2
MCM	MCM[a]	MCM[b]	calculated
MCM_a	MCM[a]	exp.[c]	calculated
MCM_b	MCM[a]	exp.[c]	constrained
FAN_a	Fantechi et al.[d]	exp.[c]	calculated
FAN_b	Fantechi et al.[d]	exp.[c]	constrained
S1	like FAN_a, with additional $RO_2 \rightarrow HO_2$ ($0.1\,s^{-1}$)		
	for RO_2 = C96CO3, FAN_D1, PINALO2, and FAN_G1		
S2	like FAN_a, with additional photolysis ($0.2 \times j_{NO2}$)		
	of first generation pinonaldehyde products		
	(4-hydroxynorpinonaldehyde, NORPINAL,		
	CO13C4CHO, CO23C4CHO, C818CO)		

[a] Master Chemical Mechanism v3.3.1

[b] Parametrization used by MCM v3.3.1

[c] Calculated from the measured solar actinic spectrum, using the absorption spectrum by Hallquist et al. (1997) and an estimated effective quantum yield of 0.9

[d] Mechanism by Fantechi et al. (2002) replaces pinonaldehyde chemistry in MCM (see Supplement)
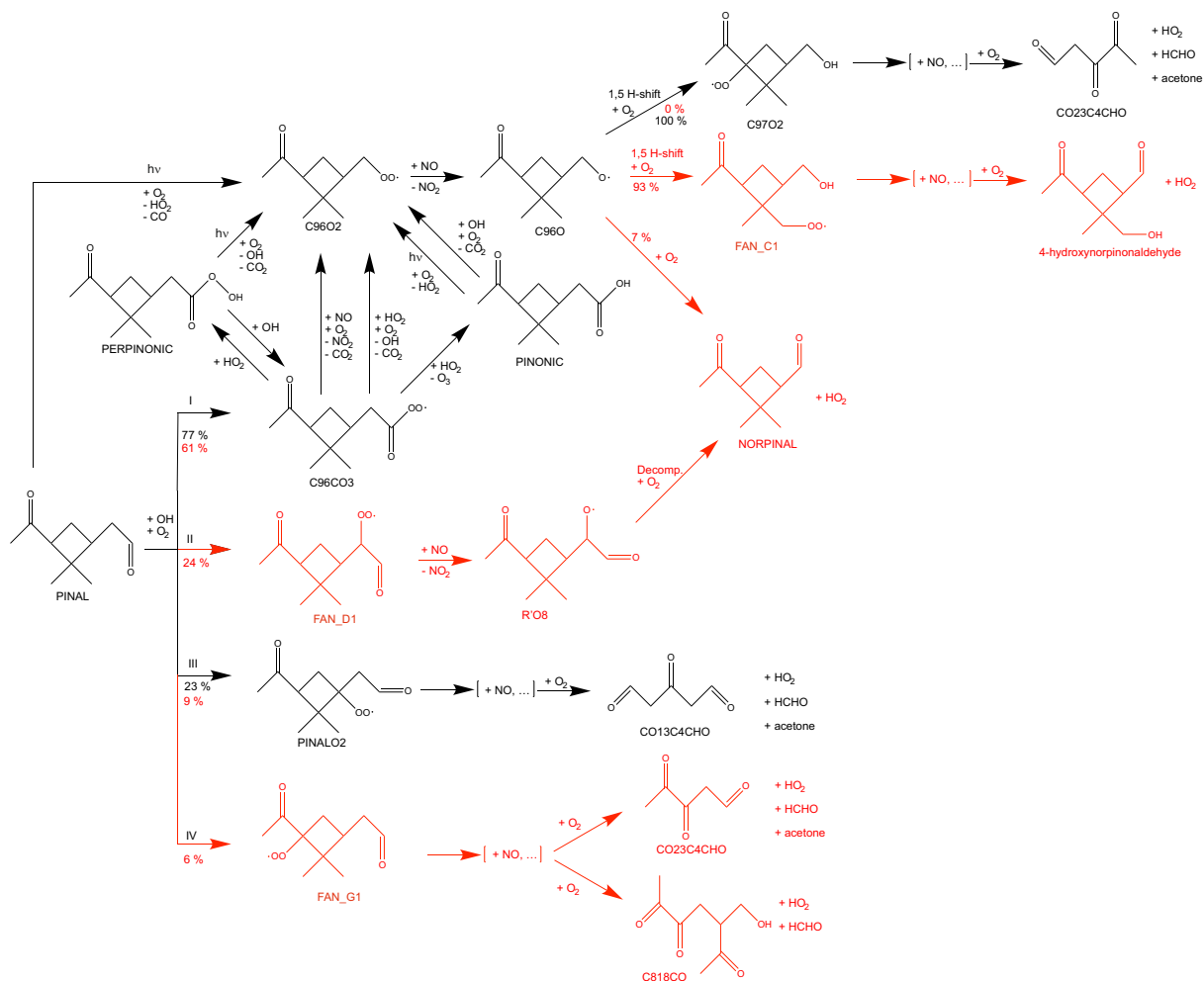
Figure 1. Simplified oxidation scheme of pinonaldehyde as described in the MCM (black) and modifications in the model derived by Fantechi et al. (2002) shown in red. [+NO, ...] represents reaction sequences which are initiated by peroxy radical reactions with NO and eventually form carbonyl compounds plus HO_2. Possible reactions of RO_2 with other RO_2 are not shown. $RO_2 + HO_2$ reactions are only shown for the major peroxy radical C96CO3. See text for details.
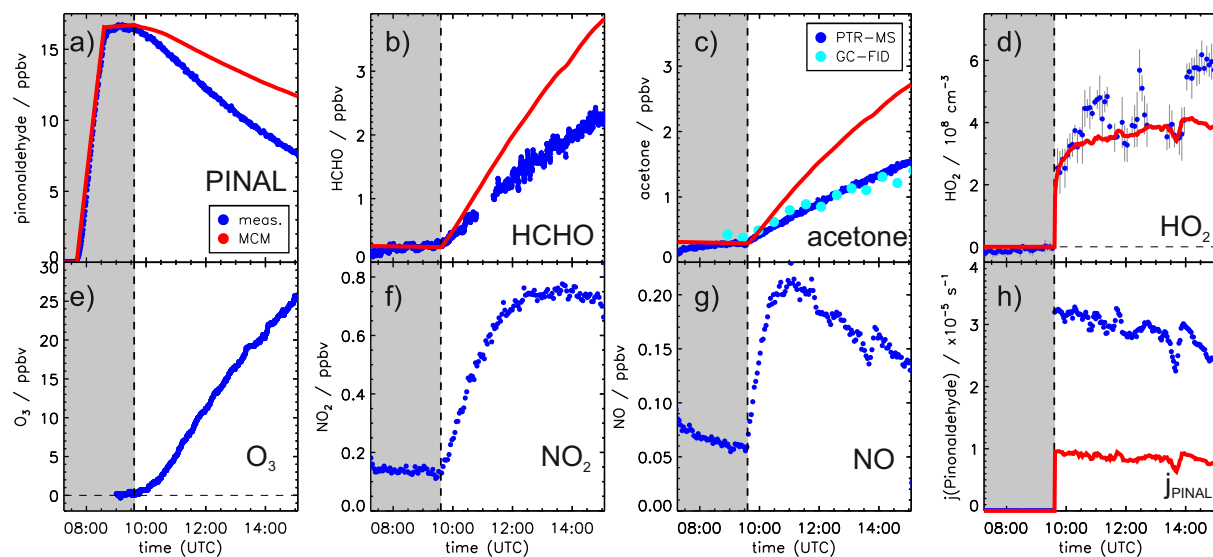
Figure 2. Measured and modeled trace gas concentrations and photolysis frequencies during photooxidation of pinonaldehyde in the presence of an OH scavenger. Pinonaldehyde is removed by photolysis, only. Measured O_3, NO_2 and NO were used as constraints for the model. See text for details of the pinonaldehyde photolysis frequency (h). Grey shaded areas indicate times when the chamber roof was closed.
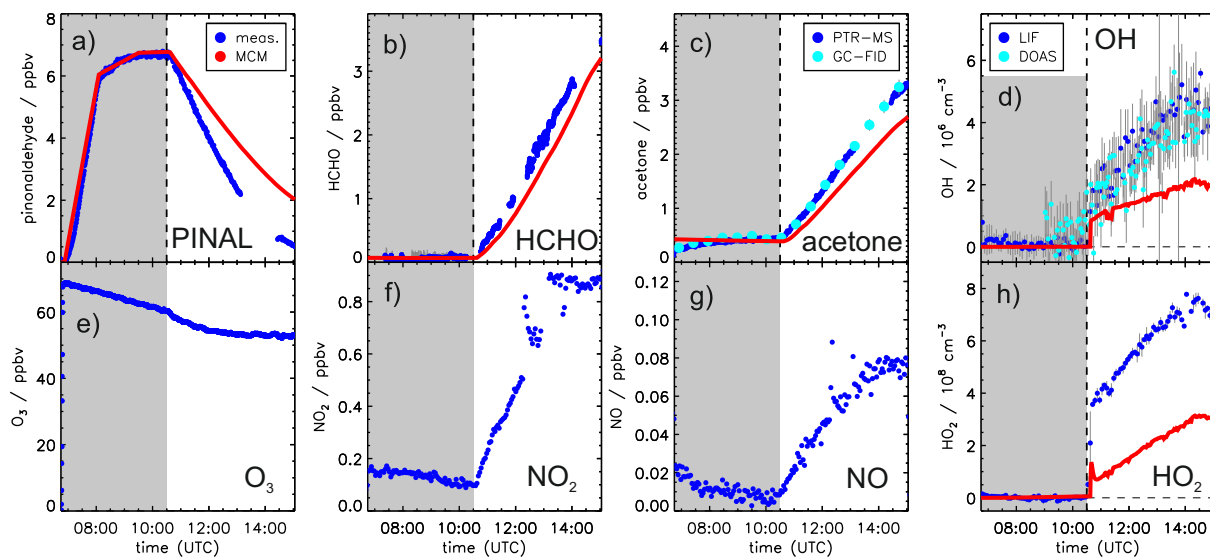
Figure 3. Measured and modeled trace gas concentrations during the photooxidation of pinonaldehyde without OH scavenger. In this experiment, pinonaldehyde is removed by photolysis and reaction with OH. Measured O_3, NO_2 and NO were used as constraints for the model. Grey shaded areas indicate times when the chamber roof was closed.
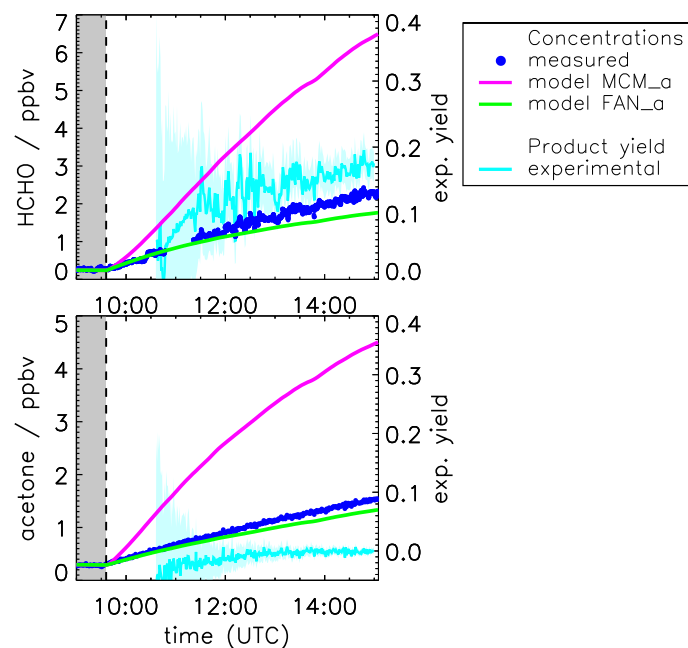
Figure 4. Measured and modeled formaldehyde and acetone mixing ratios for the experiment with OH scavenger. All model runs were done with measured photolysis frequencies for pinonaldehyde (see Fig. 6). Model runs include the MCM and the MCM with additions described in Fantechi et al. (2002). In addition, yields calculated from measured time series are shown (see text for details) with the 1σ error derived from measurements and errors of the applied correction. Colored areas give the uncertainty of this calculation. The additional error caused by the uncertainty of the chamber source is not included here.
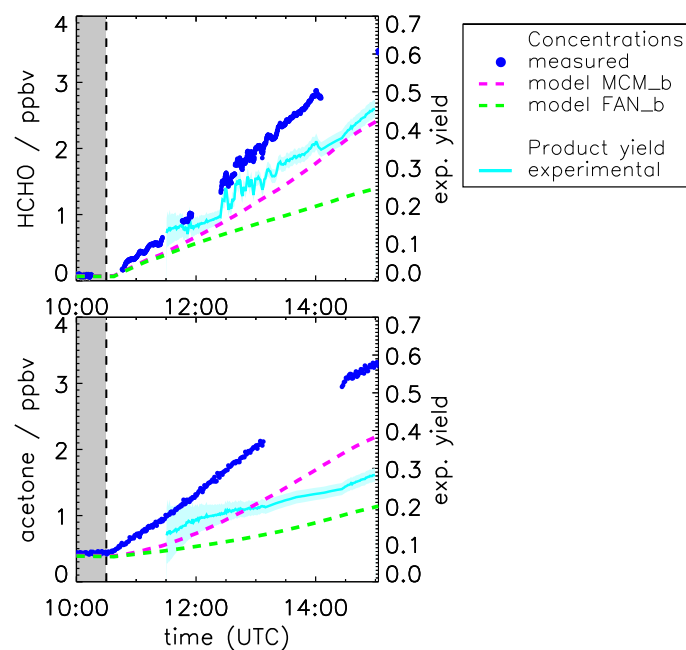
Figure 5. Measured and modeled formaldehyde and acetone mixing ratios for the experiment without OH scavenger. All model runs were done with measured photolysis frequencies for pinonaldehyde and with HO_2 constrained to measurements (see Fig. 7). Model ~~run~~ runs were done using the MCM and the MCM with modifications described in Fantechi et al. (2002). In addition, yields calculated from measured time series are shown (see text for details) with the 1σ error derived from measurements and errors of the applied correction. Colored areas give the uncertainty of this calculation. The additional error caused by the uncertainty of the chamber source is not included here.
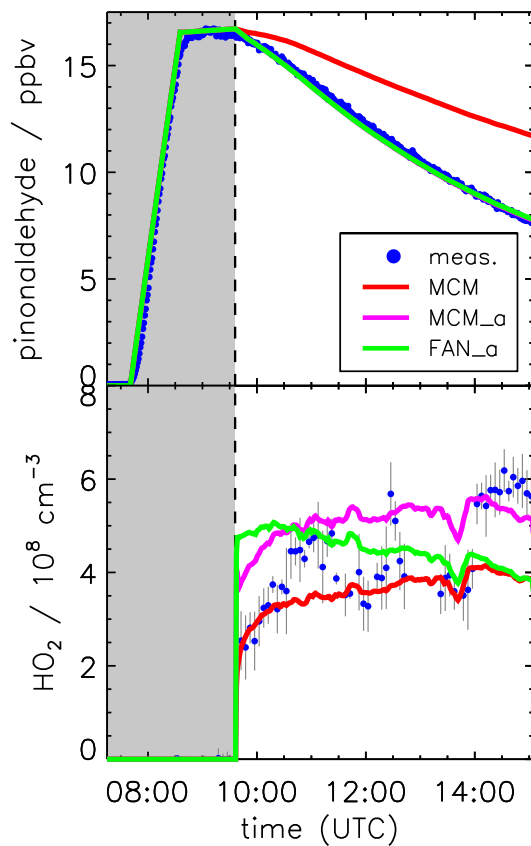
Figure 6. Pinonaldehyde and HO_2 time series during the experiment with OH scavenger. Model runs were done either using the MCM with parameterization of pinonaldehyde photolysis frequencies (MCM), with measured values for photolysis frequencies (MCM_a, see text for details) or with modifications described in Fantechi et al. (2002) (FAN_a). The pinonaldehyde concentration time profile is the same for both model runs MCM_a and FAN_a. Grey shaded areas indicate times when the chamber roof was closed.
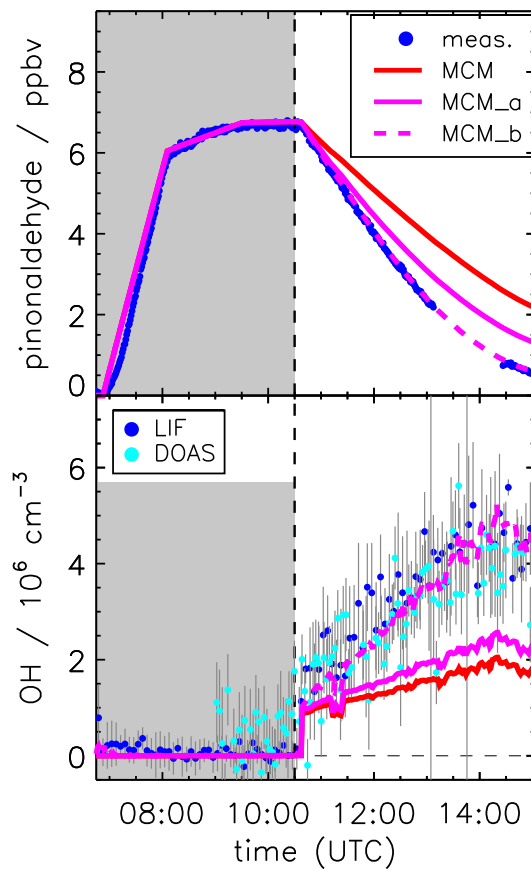
Figure 7. Pinonaldehyde and OH time series during the experiment without OH scavenger. Model runs were done either using the MCM with parameterization of pinonaldehyde photolysis frequencies (MCM) or with measured values for photolysis frequencies (MCM_a, see text for details). The model MCM_b was additionally constrained to measured HO_2 concentration, resulting in an agreement between modeled and measured (LIF and DOAS) OH concentrations. Grey shaded areas indicate times when the chamber roof was closed.
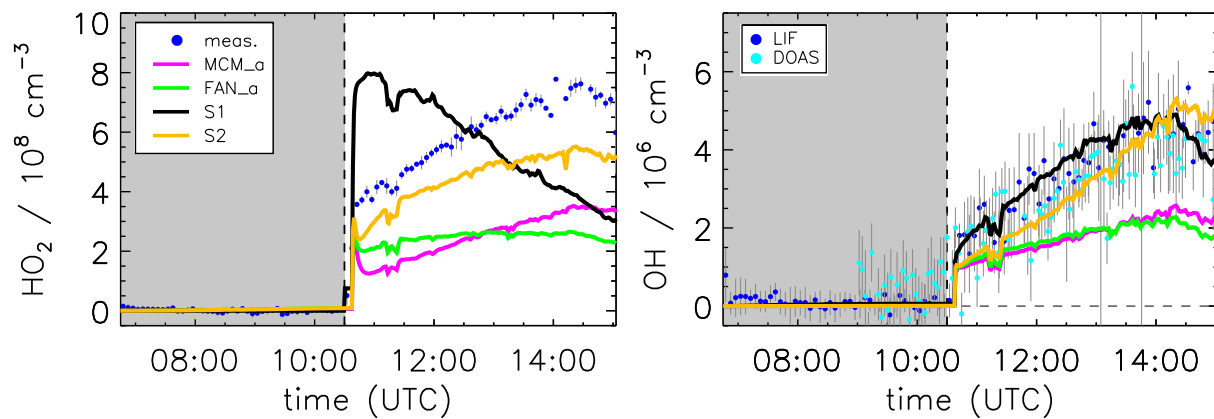
Figure 8. Model sensitivity study of the impact of potential additional HO_2 formation by unimolecular RO_2 reactions (S1) or photolysis of pinonaldehyde oxidation products (S2) compared to the model base case (MCM_a) and the case using the mechanism by Fantechi et al. (2002) (FAN_a). See Table 2 for differences in the model runs. Grey shaded areas indicate times when the chamber roof was closed.

Supplement

Model modifications based on Fantechi et al. (2002)

All additions and modifications made in the sensitivity runs Fantechi_a and Fantechi_b based on the suggestions by Fantechi et al. (2002) are shown in Table S1. The naming schema of reactants starting with an "R" is according to Fantechi et al. (2002).

In our calculations the exclusive fate of FAN_C3 is the formation of 4-hydroxynorpinonaldehyde and HO_2. Fantechi et al. (2002) state that at high NO conditions used in laboratory experiments, formic acid (HCOOH) could be formed instead.

To account for possible $RO_2 + HO_2$ reactions, a reaction scheme based on the reaction $C97O2 + HO_2$ is added for all newly introduced RO_2 species not included in the MCM. RO_2 form a corresponding hydroxyperoxide (ROOH) that can either react with OH to regenerate the RO_2 or photolyse to form the corresponding alkoxy radical (RO) that would be also formed by the reaction of $RO_2 + NO$. The general scheme is shown here for one RO_2 as an example:

$$FAN\_C1 + HO_2 \quad \rightarrow \quad FAN\_C1\_HO2 \quad (KRO2HO2) \tag{R-S1}$$

$$FAN\_C1\_HO2 + OH \quad \rightarrow \quad FAN\_C1 \quad (1 \times 10^{-11} \text{cm}^3\text{s}^{-1}) \tag{R-S2}$$

$$FAN\_C1\_HO2 + h\nu \quad \rightarrow \quad R\_O3 \quad (J_{22}) \tag{R-S3}$$

$$FAN\_C1\_HO2 + h\nu \quad \rightarrow \quad R\_O3 \quad (J_{41}) \tag{R-S4}$$
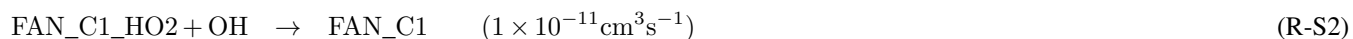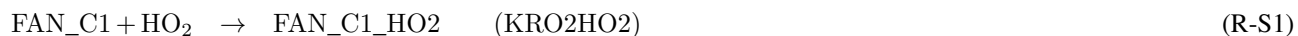
Reaction rate constants were used as stated in the MCM.

Table S1. Additional and modified reactions applied to the MCM based on the proposed mechanism by Fantechi et al. (2002). Names are taken from the MCM where existing. Newly introduced species are named either with the prefix "FAN" or "R". All nitrate species are lumped as one species RNO3.

reaction	reaction rate constant
PINAL + OH → C96CO3	$0.61 \times 5.2 \times 10^{-12} \exp(600K/T) \, cm^3 s^{-1}$
PINAL + OH → FAN_D1	$0.24 \times 5.2 \times 10^{-12} \exp(600K/T) \, cm^3 s^{-1}$
PINAL + OH → PINALO2	$0.09 \times 5.2 \times 10^{-12} \exp(600K/T) \, cm^3 s^{-1}$
PINAL + OH → FAN_G1	$0.06 \times 5.2 \times 10^{-12} \exp(600K/T) \, cm^3 s^{-1}$
C96O → NORPINAL + HO$_2$	$5.0 \times 10^4 \, s^{-1}$
C96O → FAN_C1	$6.5 \times 10^5 \, s^{-1}$
FAN_C1 + NO → R_O3 + NO$_2$	$0.86 \times$ KRO2NO[a]
FAN_C1 + NO → RNO3	$0.14 \times$ KRO2NO[a]
R_O3 → FAN_C2 + HCHO	$1.2 \times 10^7 \, s^{-1}$
R_O3 → FAN_C3	$3.2 \times 10^8 \, s^{-1}$
FAN_C2 + NO → R_O5 +NO$_2$	$0.91 \times$ KRO2NO[a]
FAN_C2 + NO → RNO3	$0.09 \times$ KRO2NO[a]
FAN_C3 → NORPINALOH + HO$_2$	$2.0 \times 10^3 \, s^{-1}$
R_O5 → FAN_C5	$0.5 \times$ KDEC[b]
R_O5 → FAN_C6	$0.5 \times$ KDEC[b]
FAN_C5 + NO → FAN_C7 + NO$_2$	$0.75 \times$ KRO2NO[a]
FAN_C5 + NO → RNO3	$0.25 \times$ KRO2NO[a]
FAN_C6 + NO → HCHO + HO$_2$ + NO$_2$	$0.93 \times$ KRO2NO[a]
FAN_C6 + NO → RNO3	$0.07 \times$ KRO2NO[a]
FAN_D1 + NO → R_O8 + NO$_2$	$0.72 \times$ KRO2NO[a]
FAN_D1 + NO → RNO3	$0.28 \times$ KRO2NO[a]
R_O8 → NORPINAL + HO$_2$	KDEC[b]
FAN_G1 + NO → FAN_G2 + NO$_2$	KRO2NO[a]
FAN_G2 + NO → R_O13 + NO$_2$	$0.89 \times$ KRO2NO[a]
FAN_G2 + NO → RNO3	$0.11 \times$ KRO2NO[a]
R_O13→ FAN_G3	$5.0 \times 10^{11} \, s^{-1}$
FAN_G3 + NO → R_O14 + NO$_2$	KRO2NO[a]
R_O14→ FAN_G4 + CO$_2$	KDEC[b]
FAN_G4 + NO → R_O15 + NO$_2$	$0.86 \times$ KRO2NO[a]
FAN_G4 + NO → RNO3	$0.14 \times$ KRO2NO[a]
R_O15→ FAN_G5	$0.5 \times 1.0 \times 10^5 \, s^{-1}$
R_O15→ FAN_G7	$0.5 \times 1.0 \times 10^5 \, s^{-1}$
FAN_G5 + NO → R_O16 + NO$_2$	$0.97 \times$ KRO2NO[a]
FAN_G5 + NO → RNO3	$0.03 \times$ KRO2NO[a]
R_O16→ C818CO + HCHO + HO$_2$	KDEC[b]
FAN_G7 + NO → R_O17 + NO$_2$	$0.97 \times$ KRO2NO[a]
FAN_G7 + NO → RNO3	$0.03 \times$ KRO2NO[a]
R_O17→ CO23C4CHO + CH3COCH3 + HO$_2$	KDEC[b]

[a] value from MCM: KRO2NO= $2.7 \times 10^{-12} \exp(360K/T) \, cm^3 s^{-1}$ (MCM, 2017)
[b] value from MCM: KDEC= $1.0 \times 10^6 \, s^{-1}$ (MCM, 2017)

Sensitivity study S1 and additional sensitivity tests

In S1 the impact of hypothetical isomerization reactions of all 4 initially formed RO_2 radicals on model results was tested. Reactions shown in Tab. S2 were added to the model based on Fantechi et al. (2002). Possible isomerziation reactions in later stages of the mechanism were not tested.

Table S2. Overview of added reactions for sensitivity run S1.

reaction	reaction rate constant
$C96CO3 \rightarrow HO_2$	$0.1\,s^{-1}$
$PINALO2 \rightarrow HO_2$	$0.1\,s^{-1}$
$FAN\_D1 \rightarrow HO_2$	$0.1\,s^{-1}$
$FAN\_G1 \rightarrow HO_2$	$0.1\,s^{-1}$

However, only PINALO2, FAN_D1, and FAN_G1 have an aldehyde group with a hydrogen that can be easily abstracted. An additional sensitivity study (S1_mod) was performed that includes only isomerization reactions of these 3 RO_2 applying the same reaction rates used for S1. Figure S1 shows the calculated HO_2 and OH time series together with results from S1, model base case (MCM_a), and modified mechanism by Fantechi et al. (2002) (FAN_a).

Figure S1. Model sensitivity studies of the impact of potential additional HO_2 formation by unimolecular RO_2 reactions of all 4 initial RO_2 (S1) and for RO_2 radicals with a –HCO group (S1_mod). The sensitivity test S1_mod_hv extends S1_mod by an additional photolysis of isomerization products. In addition, the model base case (MCM_a) and the case using the mechanism by Fantechi et al. (2002) (FAN_a) are shown. Grey shaded areas indicate times when the chamber roof was closed.

These RO_2 radicals are formed with a yield of 39 %. Therefore, HO_2 concentrations in the beginning of the experiment are reduced by a factor of 2 compared to S1 where the isomerization of all initial RO_2 leads to the formation of HO_2. The reduced HO_2 concentrations agree with observations at the start of the photooxidation, but show the same temporal trend as in model run S1 over the course of the experiment. This leads to an increasing model-measurement discrepancy of HO_2 concentrations of a factor of up to 3. Consistently, OH concentrations are reduced by a factor of 2 compared to S1.

Products of the rapid isomerization reaction could be peroxy acids with additional carbonyl functions. As seen for pinonalde-hyde, photolysis frequencies of bi-carbonyl compounds could be generally underestimated in current models. An additional sensitivity test (S1_mod_hv) with isomerization of initially formed RO_2 with –HCO group followed by photolysis of the iso-

merization products with the photolysis frequency of glyoxal was performed. Because the photolysis frequency of glyoxal is slow compared to the reaction rate of the isomerization reaction, the HO_2 concentration time series in this sensitivity model run is similar to the sensitivity run with only isomerization (S1_mod). The formation of HO_2 is linked to the RO_2 concentration in this case and underestimated by the model.

Sensitivity test of $RO_2 + NO$ reaction rate constants
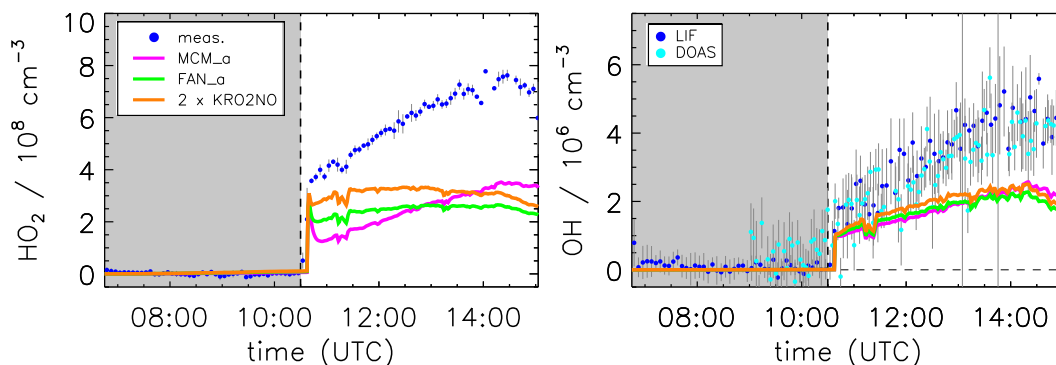
Figure S2. Model sensitivity run with modified reaction rate of 2xKRO2NO. The modified reaction rate constant was applied to all RO_2 that were introduced by the model modifications based on Fantechi et al. (2002). Grey shaded areas indicate times when the chamber roof was closed.

Sensitivity study S3

In the used mechanism based on Fantechi et al. (2002) 4-hydroxynorpinonaldehyde was formed as main product with an overall yield of approximately 25 % but no subsequent chemistry was considered in the MCM model and the modified Fantechi mechanism. To investigate if the subsequent chemistry of this product has the potential to partly explain the missing HO_2 source a mechanism was deduced from structure–activity relationship (SAR; Kwok and Atkinson, 1995; Vereecken and Peeters, 2009; Vereecken and Nozière, 2020). No theoretical calculations were performed.
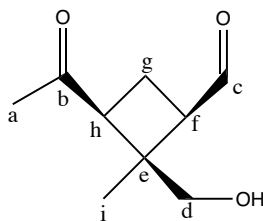
Figure S3. Structure of 4-hydroxynorpinonaldehyde and C-atom labeling.

The 4-hydroxynorpinonaldehyde structure is shown in Fig. S3. Reaction rate constants for the H-abstraction by OH were estimated based on Kwok and Atkinson (1995) and are shown in Table S3.

Table S3. Reaction rate constants for H-abstraction by OH for different carbon atoms based on Kwok and Atkinson (1995).

C-atom	reaction rate constant	fraction
c	$1.69 \times 10^{-11}\,\mathrm{cm^3\,s^{-1}}$	79 %
d	$3.27 \times 10^{-12}\,\mathrm{cm^3\,s^{-1}}$	15 %
f	$5.43 \times 10^{-13}\,\mathrm{cm^3\,s^{-1}}$	3 %
g	$2.62 \times 10^{-13}\,\mathrm{cm^3\,s^{-1}}$	1 %
h	$5.43 \times 10^{-13}\,\mathrm{cm^3\,s^{-1}}$	3 %

A simplified mechanism of the subsequent degradation of 4-hydroxynorpinonaldehyde is shown in S4. An overview of added reactions is shown in Tab. **??**. Reaction rates are base on Vereecken and Peeters (2009); Vereecken and Nozière (2020). Only the main reaction branches ($\geq 5\%$) were investigated. The mechanism was constructed according to Jenkin et al. (1997). For all $RO_2 + NO$ reactions the standard reaction rate from MCM (KRO2NO) and an organic nitrate yield of 23 % was used. $RO_2 + HO_2$ reactions were included as described for the modified mechanism based on Fantechi et al. (2002). The photolysis frequency of pinononaldehyde was used for the photolysis of formed hydroperoxides (ROOH).

H-abstraction by OH mainly occurs at the aldehyde group forming the peroxy radical C1. After a rapid CO_2 elimination, C1 forms C2 and C3 in equal amounts. C2 can undergo an 1,5 H-shift to form a stable hydroperoxy compound (C5) and HO_2. Alternatively, C2 can form the alkoxy radical C4 after reaction with NO. Similarly, C3 forms the alkoxy radical C12. Ring-opening of the 4-membered ring in both C4 and C12 leads to the formation of a peroxy radical C6. Subsequently, the main fraction (approximately 90 %) rearranges after an 1,6 H-shift to C9. C9 either undergoes an 1,6 H-shift forming C10 or forms an alkoxy radical that further decomposes to a stable product and HO_2.

A sensitivity run (S3) using the degradation scheme of 4-hydroxynorpinonaldehyde was performed and results can be seen in Fig. S5. The modifications have only a small effect on HO_2 and OH concentrations. In the second half of the experiment the degradation of pinonaldehyde oxidation products becomes more relevant and additional HO_2 is formed by the 4-hydroxynorpinonaldehyde degradation scheme. However, the effect on the HO_2 concentration is small and HO_2 concentrations are increased by up to 10 % compared to FAN_a."
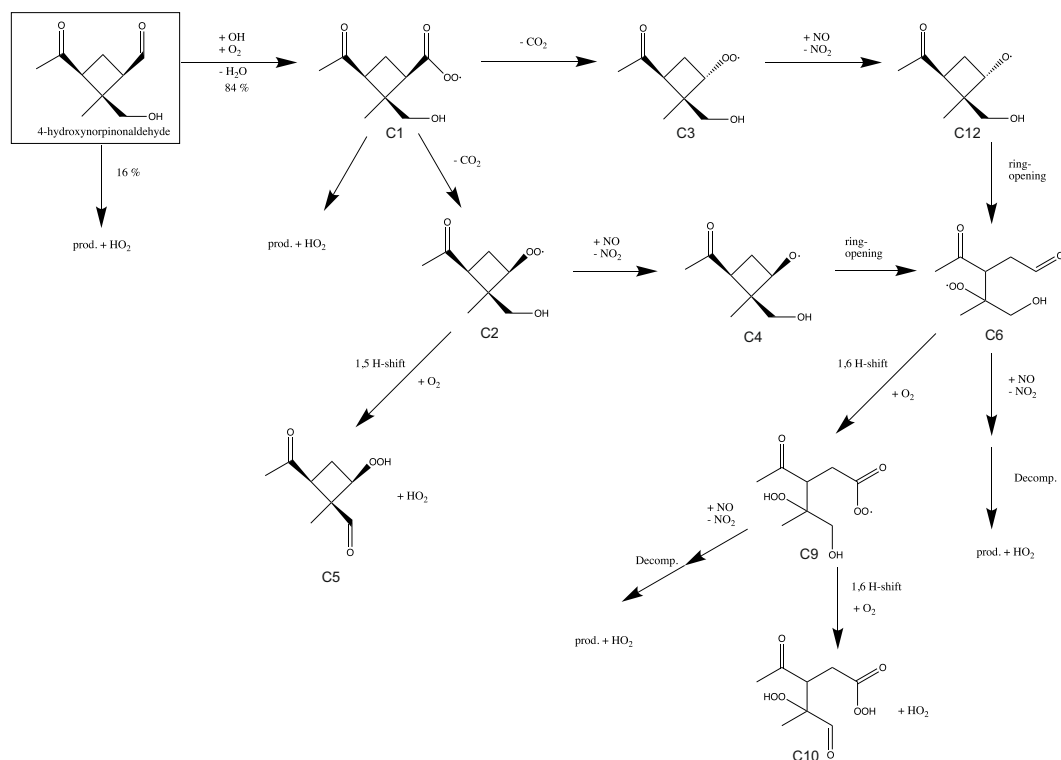
Figure S4. Simplified mechanism of the subsequent degradation of 4-hydroxynorpinonaldehyde. The mechanism is deduced from SAR. For details see text. $RO_2 + HO_2$ reactions and $RO_2 + NO$ reactions that form nitrates are not shown.
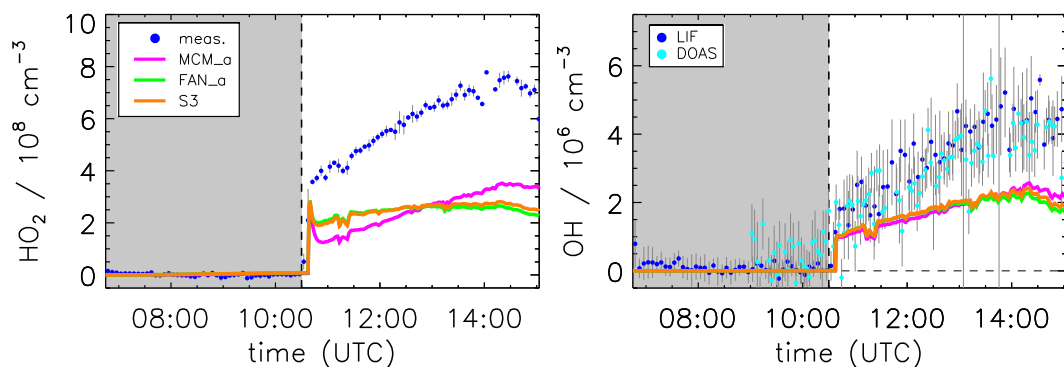
Figure S5. Model sensitivity study of the impact of a 4-hydroxynorpinonaldehyde degradation mechanism (S3) compared to the model base case (MCM_a) and the case using the mechanism by Fantechi et al. (2002) (FAN_a). Grey shaded areas indicate times when the chamber roof was closed.

Table S4. Extended mechanism for the further degradation of 4-hydroxynorpinonaldehyde used for sensitivity test S3. For details see text. All nitrate species are lumped as one species RNO3.

reaction	reaction rate constant
NORPINALOH + OH → C1	1.69×10^{-11} cm^3 s^{-1} [a]
NORPINALOH + OH → D1 + HO$_2$	3.27×10^{-12} cm^3 s^{-1} [a]
NORPINALOH + OH → F1 + HO$_2$	5.43×10^{-13} cm^3 s^{-1} [a]
NORPINALOH + OH → G1 + HO$_2$	2.62×10^{-13} cm^3 s^{-1} [a]
NORPINALOH + OH → H1 + HO$_2$	5.43×10^{-13} cm^3 s^{-1} [a]
NORPINALOH + hν → C2 + HO$_2$	j_{PINAL}
C1 → C2 + CO$_2$	KDEC[b]
C1 → C3 + CO$_2$	KDEC[b]
C1 → prod. + HO$_2$	9.16×10^{-2} s^{-1}
C1 + NO → C1O + NO$_2$	0.77*KRO2NO[c]
C1 + NO → RNO3	0.23*KRO2NO[c]
C1 + HO$_2$ → C1OOH	KRO2HO2[d]
C1OOH + OH → C1	1.3×10^{-11} cm^3 s^{-1}
C1OOH + hν → C1O + OH	j_{PINAL}
C1O → prod. + HO$_2$	KDEC[b]
C2 + NO → C4 + NO$_2$	0.77*KRO2NO[c]
C2 + NO → RNO3	0.23*KRO2NO[c]
C2 → C5 + HO$_2$	1.3×10^{-2} s^{-1}
C2 + HO$_2$ → C2OOH	KRO2HO2[d]
C2OOH + OH → C2	1.3×10^{-11} cm^3 s^{-1}
C2OOH + hν → C4 + OH	j_{PINAL}
C4 → C6	KDEC[b]
C6 → C9	2.8×10^{-1} s^{-1}
C6 + NO → C7 + NO$_2$	0.77*KRO2NO[c]
C6 + NO → RNO3	0.23*KRO2NO[c]
C6 + HO$_2$ → C6OOH	KRO2HO2[d]
C6OOH + OH → C6	1.3×10^{-11} cm^3 s^{-1}
C6OOH + hν → C7 + OH	j_{PINAL}
C7 → C8 + ACETOL	KDEC[b]
C8 → prod. + HO$_2$	KDEC[b]
C9 → C10 + HO$_2$	6.6×10^{-4} s^{-1}
C9 + NO → C11 + NO$_2$	0.77*KRO2NO[c]
C9 + NO → RNO3	0.23*KRO2NO[c]
C9 + HO$_2$ → C9OOH	KRO2HO2[d]
C9OOH + OH → C9	1.3×10^{-11} cm^3 s^{-1}
C9OOH + hν → C11 + OH	j_{PINAL}
C11 → C13 + HO$_2$	KDEC[b]
C3 + NO → C12 + NO$_2$	0.77*KRO2NO[c]
C3 + NO → RNO3	0.23*KRO2NO[c]
C3 + HO$_2$ → C3OOH	KRO2HO2[d]
C3OOH + OH → C3	1.3×10^{-11} cm^3 s^{-1}
C3OOH + hν → C12 + OH	j_{PINAL}
C12 → C6 + HO$_2$	KDEC[b]

[a] value from Kwok and Atkinson (1995)
[b] value from MCM: KDEC$= 1.0 \times 10^6$ s^{-1} (MCM, 2017)
[c] value from MCM: KRO2NO$= 2.7 \times 10^{-12}$ exp(360K/T) cm^{3}s^{-1} (MCM, 2017)
[d] value from MCM: KRO2HO2$= 2.91 \times 10^{-13}$ exp(1300K/T) cm^{3}s^{-1} (MCM, 2017)

Sensitivity test of additional acetone and HCHO formation by pathways II, III, and IV

In a sensitivity study it was tested if the pathways II, III, and IV that do not form 4-hydroxynorpinonaldehyde have the potential to explain the missing acetone and formaldehyde formation in the OH oxidation experiment. In a sensitivity test the first reaction step of the pathways II, III, and IV form one molecule of acetone and HCHO each. Results are shown in Fig. S6. The additional acetone and HCHO sources can reproduce observations in the first half of the experiment within the measurement uncertainty when contributions from OH reactions of product species are small. In later stages of the experiment, acetone and formaldehyde concentrations are underestimated by the sensitivity model run. Additional acetone and HCHO formation from further degradation of oxidation products not included in the MCM could explain the model-measurement discrepancy. See the response to comment 4 for more information of potential products of the degradation of 4-hydroxinorpinonaldehyde.
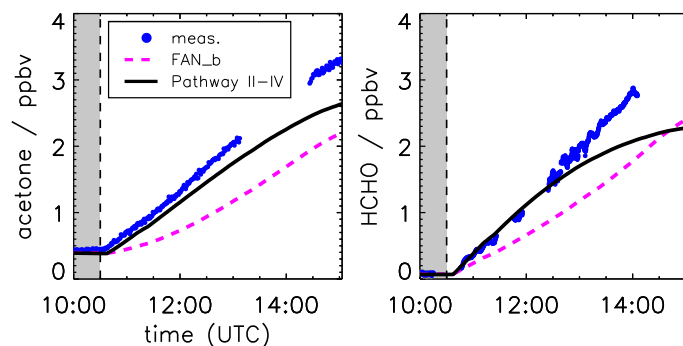
Figure S6. Measured and modeled formaldehyde and acetone mixing ratios for the experiment without OH scavenger. All model runs were done with measured photolysis frequencies for pinonaldehyde and with HO_2 constrained to measurements. Model runs were done using modifications described in Fantechi et al. (2002). For the model run shown in black an additional HCHO and acetone formation in pathways II, III, and IV is assumed.

References

Fantechi, G., Vereecken, L., and Peeters, J.: The OH-initiated atmospheric oxidation of pinonaldehyde: Detailed theoretical study and mechanism construction, Phys. Chem. Chem. Phys., 4, 5795–5805, https://doi.org/10.1039/B205901K, 2002.

Jenkin, M. E., Saunders, S. M., and Pilling, M. J.: The tropospheric degradation of volatile organic compounds: A protocol for mechanism development, Atmos. Environ., 31, 81–104, https://doi.org/10.1016/S1352-2310(96)00105-7, 1997.

Kwok, E. S. C. and Atkinson, R.: Estimation of hydroxyl radical reaction rate constants for gas-phase organic compounds using a structure-reactivity relationship: An update, Atmos. Environ., 29, 1685–1695, https://doi.org/10.1016/1352-2310(95)00069-B, 1995.

MCM: Master Chemical Mechanism, http://mcm.leeds.ac.uk/MCM/, last access: 04 March 2020, 2017.

Vereecken, L. and Nozière, B.: H migration in peroxy radicals under atmospheric conditions, Atmos. Chem. Phys., 20, 7429–7458, https://doi.org/10.5194/acp-20-7429-2020, 2020.

Vereecken, L. and Peeters, J.: Decomposition of substituted alkoxy radicals-part I: a generalized structure-activity relationship for reaction barrier heights, Phys. Chem. Chem. Phys., 11, 9062–9074, https://doi.org/10.1039/B909712K, 2009.